Reply to the RC: Inter-comparison and improvement of 2-stream shortwave radiative transfer models for unified treatment of cryospheric surfaces in ESMs

April 2019

We thank the Editor and two Reviewers for their insightful comments that have led to material improvements in the manuscript. To avoid confusion, we have replaced CICE with dEdd-AD to refer the radiative transfer core of sea-ice models; we have included one extra table (Table 1) to summarize the acronyms used in this work. We also changed the paper title from "*Inter-comparison and improvement of 2-stream shortwave radiative transfer models for unified treatment of cryospheric surfaces in ESMs*" to "*Inter-comparison and improvement of **two-stream** shortwave radiative transfer models **in ESMs** for **a** unified treatment of cryospheric surfaces*".

Please find our replies to the questions and suggestions raised by the Reviewers below.

Anonymous Referee #1

This paper aims to unify the treatment of the optical properties of snow and ice in ESMs, because, historically, there have often been different albedo schemes in one and the same ESM, applied to seasonal snow, snow on sea ice, and snow on land ice masses like ice sheets. In particular, the authors focus on SNICAR (used for land ice and land masses), and Icepack/CICE (for sea ice). All radiative transfer schemes in ESMs are two-stream approximations. They assess the accuracy of the 2-stream approximations of different flavors against DISORT in a 16-stream configuration and consider this as the benchmark. I have few comments on the research itself. This is solid and has been carefully designed, and conducted. I do have critical remarks on the presentation of the results. They are surprisingly unclear in a few key parts, to the extent that I am unsure what the authors have actually done and what they haven't done.

The problem lies in the fact that there is (1) a correction for high SZA > 75 degrees, and (2) mention of a hybrid model SNICAR-AD. To me it is unclear whether these are the same thing or not. The high-SZA correction seems to be carried out on CICE rather than SNICAR. The authors suggest that a correction (equations 13 a and b) can be conducted for any 2-stream approximation, so also for SNICAR. So what is the situation after this paper? Do the authors now have 1 model for all snow and ice surfaces? Or did they present a correction for CICE only? Or also for SNICAR? And is this then SNICAR-AD? And what are the recommendation in section 8 about? Is this for future work? Or are these points that have been taken into account while a unified model framework was developed?

All in all, there are two possibilities: (1) either the authors have forgotten to mention that the correction for SZA > 75 degrees is actually called SNICAR-AD. In that case, Figure 12 needs different figure axis labels and the text needs to clarify that this correction is called SNICAR-AD in a few places. In this case, I would suggest to move section 8 forward between the current sections 5 and 6, so as to present first the requirements for a unified model, and then the actual unified model. Or, (2) the correction for SZA > 75 degrees is not the same as SNICAR-AD, but rather an intermediate step in the unification of Icepack and SNICAR. In that case, the paper is incomplete. Results from the to-be-developed SNICAR-AD need to be incorporated here. If this would be paper 1 presenting the SZA-correction, and in a future paper 2 we will see SNICAR-AD fully developed, then I recommend that this paper is postponed to when SNICAR-AD is finished. I recommend to the editor to inquire with the authors which of these possible situations is the case, and then reach a decision.

Reply: We thank the Reviewer for their questions and suggestions. We have revised Sections 6 and 8 to address these concerns and to clarify our work.

First of all, SNICAR-AD is the unified treatment that we developed by merging SNICAR with dEdd-AD (note dEdd-AD was referred to as CICE in version 1, and is now called dEdd-AD in version 2 following the Reviewer's suggestion), and incorporating our correction for SZA > 75 degrees. We have finished the development of this scheme, and we are testing its performance using E3SM. To make this point clear, we added the following text in Section 8:

Lines 870-882: "We have merged these findings into a hybrid model SNICAR-AD, which is primarily composed of the radiative transfer scheme of dEdd-AD, 5-band snow/aerosol SSPs of SNICAR, and the parameterization to correct for snow albedo biases when solar zenith angle exceeds 75°. This hybrid model can be applied to snow on land, land ice, and sea ice to produce consistent shortwave radiative properties for snow-covered surfaces across the Earth system. With the evolving and further understanding of snow and aerosol physics and chemistry, the adoption of this hybrid model will obviate the effort to modify and maintain separate optical variable input files used for different model components.

SNICAR-AD is now implemented in both the sea-ice (MPAS-seaice) and land (ELM) components of E3SM. More simulations and analyses are underway to examine its impact on E3SM model performance and simulated climate. The results are however beyond the scope of this work and will be thoroughly discussed in a future paper."

Second, the high-SZA correction applies in principle to any two-stream algorithms, including SNICAR and dEdd-AD (i.e. CICE in version 1). In Section 6, we introduced the high-SZA correction using dEdd-AD (i.e. CICE in version 1) assuming dEdd-AD will be the radiative transfer core used for all snow-covered surface per discussed in Section 8. The Reviewer's concern is however crucial since the adjustment factor R_{75+} is essentially a ratio of the exact reflectance to the two-stream reflectance, which is algorithm-specific,

$$R_{75+} = \frac{\alpha_{16-DISORT}}{\alpha_{dEdd-AD}}$$

We have included more discussion to make this point clear:

Lines 590-595: "For solar zenith angles > 75°, two-stream models underestimate snow albedo and overestimate solar absorption within snowpack, mostly in the top 2-cm of snow, and the differences among three two-stream models are small. In Section 5, we have shown that dEdd-AD produces the most accurate snow albedo in general, with anticipated wide application of dEdd-AD, we develop the following parameterization to adjust its low biases in computed near-IR direct albedo."

Lines 631-661: "When the solar zenith angle exceeds 75°, our model adjusts the computed direct near-IR albedo $\alpha_{dEdd\text{-}AD}$ by the ratio R_{75+} following equations 12-14a and reduces direct near-IR absorption following equation 14b. If snow is divided into multiple layers, we assume all decreased near-IR absorption (2nd term on the right hand side, equation 14b) is confined within the top layer. This assumption is fairly accurate for the near-IR band, since most absorption occurs at the surface of snowpack (Figures 10 and 11). As discussed previously, this parameterization is developed based on albedo computed using dEdd-AD. For models that do not use dEdd-AD but SNICAR and 2SD, the same adjustment still applies given the small differences of near-IR direct albedo computed using two-stream models (Figure 11). For models that adopt other radiative transfer algorithms it is best for the developers to examine their model against a benchmark model such as 16-stream DISORT or two-stream models discussed in this work before applying this correction."

Thirdly, Section 8 summarizes the findings of this work, which are essentially the principles we follow to generate the merged model SNICAR-AD. We hope that the discussion and recommendations in this section are also useful to readers who are interested in improving their own snow radiative transfer schemes besides SNICAR or dEdd-AD. Some of the discussion includes future directions and features that are not yet included in SNICAR-AD, such as increasing the number of bands to match RRTMG. The revised text in section 8 reflects the above discussion.

Referee #2
David Bailey (dbailey@ucar.edu)

I have read the manuscript: "Inter-comparison and improvement of 2-stream shortwave radiative transfer models for a unified treatment of cryospheric surfaces in ESMs" by Dang et al. Overall, the article is interesting and may be of interest to the readers of the Cryosphere. I believe it needs some substantial revision before it would be acceptable however. There are a lot of model acronyms thrown around here and the text should be expanded to help clarify in some sections. Also, I feel it is lacking a bit in motivation. I understand from the title, the idea is to unify the radiative transfer schemes for snow on land, ice sheets, and sea ice, but a bit more here would be good. For example: Is it easier to maintain? Is there performance benefits? Does the accurate simulation of surface albedo matter for climate given the small differences between the algorithms here? The text also needs some significant grammar checking.

Reply: Thank you for these suggestions and questions.

To help clarify these models, we add a new table (Table 1 in the revised manuscript) to summarize the acronyms and their corresponding references used in this work.

Yes. It is easier to maintain an ESM with the unified scheme than with distinct schemes in the land and sea-ice components. For example, CICE-based sea-ice models utilize hardcoded snow single-scattering properties that are not easy to update, and that yield different reflectance and heating than SNICAR-based properties. With this unified treatment, an Earth system model only needs to maintain and update a single input optical data file shared by both land and sea-ice components. As our evaluations show, the adoption of dEdd-AD radiative transfer core, SNICAR single-scattering properties, and the high solar zenith angle parameterization improves the modeled physics.

The accurate simulation of surface albedo matters despite the apparently small differences between the algorithms. For example, compared to dEdd-AD, SNICAR and 2SD overestimate the diffuse albedo of melting snow by 0.015 (Figure 6). In Greenland, the daily-averaged downward diffuse solar flux from May to September is 200W/m 2, and the mean cloud cover fraction is 80% (Figure 6, Dang et al., 2017). In this case, SNICAR and 2SD overestimate the reflected solar flux by 0.015 * 200* 0.8 ~ 2.4 W/m^2, which is enough to melt 10 cm SWE over all of Greenland from May to September. dEdd-AD also remediates self-compensating spectral biases (where visible and Near-IR biases are of opposite signs) present in the other schemes. Those spectral biases do not affect the broadband fluxes like the diffuse biases, but they nevertheless degrade proper feedbacks between snow/ice reflectance and heating. To better evaluate these impacts globally, we are now performing coupled E3SM simulations. The results will be discussed in a following paper.

More discussion is included in Section 8 to clarify these points.

Lines 525-521: "These relatively small differences between algorithms may still yield large impact on snowpack. For example, compared to dEdd-AD, SNICAR and 2SD overestimate the diffuse albedo by ~0.015 for melting snow (Figure 6). In Greenland, the daily averaged downward diffuse solar flux from May to September is 200 W/m^2, and the averaged cloud cover fraction is 80% (Figure 6, Dang et al., 2017). In this case, SNICAR and 2SD overestimate the reflected solar flux by 2.4 W/m^2 per day – the amount of energy otherwise enough to melt 10 cm of snow water equivalent from May to September. dEdd-AD also remediates self-compensating spectral biases (where visible and Near-IR biases are of opposite signs) present in the other schemes. Those spectral biases do not affect the broadband fluxes like the diffuse biases, but they nevertheless degrade proper feedbacks between snow/ice reflectance and heating."

Lines 870-882: "We have merged these findings into a hybrid model SNICAR-AD, which is primarily composed of the radiative transfer scheme of dEdd-AD, 5-band snow/aerosol SSPs of SNICAR, and the parameterization to correct for snow albedo biases when solar zenith angle exceeds 75°. This hybrid model can be applied to snow on land, land ice, and sea ice to produce consistent shortwave radiative properties for snow-covered surfaces across the Earth system. With the evolving and further understanding of snow and aerosol physics and chemistry, the adoption of this hybrid model will obviate the effort to modify and maintain separate optical variable input files used for different model components.

SNICAR-AD is now implemented in both the sea-ice (MPAS-seaice) and land (ELM) components of E3SM. More simulations and analyses are underway to examine its impact on E3SM model performance and simulated climate. The results are however beyond the scope of this work and will be thoroughly discussed in a future paper"

Here are some more specific suggestions:

1. It is very confusing when the delta-Eddington radiative transfer scheme of Briegleb and Light (2007) is interchangeably referred to as CICE, Icepack, delta-Eddington, adding-doubling delta-Eddington, etc. I suggest you just refer to it as dEdd everywhere and clearly explain that you are talking about the default implementation of Briegleb and Light (2007) and not some modified version?

Reply: Thank you for this suggestion. We agree that using dEdd for sea-ice component is better than CICE since this is also the name of sea-ice radiative transfer scheme defined in Icepack/CICE/MPAS-seaice model namelist. The use of dEdd everywhere may, however, raise another confusion since SNICAR also adopts two-stream delta-Eddington approximation for snow visible optical properties, but with a different technique per discussed in Section 2. To distinguish the scheme of Briegleb and Light (2007) from what is implemented in SNICAR, we suggest referring to it as dEdd-AD, where AD is short for adding-doubling and corresponds to the AD in the name of the unified model SNICAR-AD. We have revised the related text, figures, and tables to reflect this change. We apply the default implementation of Briegleb and Light (2007) to snow in this work, which is stated in Section 2.2.

2. The first sentence of the abstract should say something more quantitative than "large

parts of the Earth".

Reply: Thank you. We have revised it as "mid and high latitudes of the Earth".

3. The first two paragraphs should mention melt ponds and meltwater in the snow. These are critical for the seasonal cycle evolution of albedo.

Reply: Agreed. We now discuss snow melt in the first paragraph.

Lines 46-50: "The accumulation, evolution, and depletion of snow cover modify the seasonal cycle of surface albedo globally. In particular, snow over sea ice absorbs more solar energy and begins to melt in the spring, which forms melt ponds that bring the sea-ice albedo to as low as 0.15 to further accelerate ice melt (Light et al., 2008, 2015)."

4. Line 116: "This method has carried into the sea-ice..." This is not proper usage.

Reply: We have modified this sentence:

Lines 127-130: "dEdd-AD has been adopted by the sea-ice physics library Icepack (https://github.com/CICE-Consortium/Icepack/wiki), which is used by the Los Alamos Sea Ice Model CICE (Hunke et al., 2010) and Model for Prediction Across Scales Sea Ice MPAS-seaice (Turner et al., 2018)."

5. The discussion of large solar Zenith angles is an interesting part. I think some suggestions of ways to improve how the models do this is needed.

Reply: Thank you for the suggestion. We have modified section 6 to include more details on how to implement the adjustment when the solar zenith angles exceed 75 degrees:

Lines 631-661: "When the solar zenith angle exceeds 75°, our model adjusts the computed direct near-IR albedo $\alpha_{dEdd\text{-}AD}$ by the ratio R_{75+} following equations 12-14a and reduces direct near-IR absorption following equation 14b. If snow is divided into multiple layers, we assume all decreased near-IR absorption (2nd term on the right hand side, equation 14b) is confined within the top layer. This assumption is fairly accurate for the near-IR band, since most absorption occurs at the surface of snowpack (Figures 10 and 11). As discussed previously, this parameterization is developed based on albedo computed using dEdd-AD. For models that do not use dEdd-AD but SNICAR and 2SD, the same adjustment still applies given the small differences of near-IR direct albedo computed using two-stream models (Figure 11). For models that adopt other radiative transfer algorithms it is best for the developers to examine their model against a benchmark model such as 16-stream DISORT or two-stream models discussed in this work before applying this correction."

6. Some mention of how the methods handle aerosols (black carbon and dust) would be good. For example, see Holland et al. 2012: https://journals.ametsoc.org/doi/10.1175/JCLI-D-11-00078.1

Reply: Thank you for this suggestion and reference. Aerosol-in-snow/ice is definitely one of the topics we are interested in. Currently, we are performing fully coupled E3SM simulations to quantify the radiative effects of aerosols in the cryosphere with SNICAR-AD. The analysis of these modeled results will serve the same purpose as Holland et al., 2012. We anticipate some change in the radiative effects of aerosols, but the unified model SNICAR-AD does not change how the snow model treats aerosols. The discussion can be found towards the end of Section 8:

Lines 843-857: "Both dEdd-AD and SNICAR simulate the impact of light-absorbing particles (black carbon and dust) on snow and/or sea ice using self-consistent particle SSPs that follow the SNICAR convention (e.g., Flanner et al., 2007; Holland et al. 2012). These particles are assumed to be either internally or externally mixed with snow crystals; the combined SSPs of mixtures (e.g. Appendix A of Dang et al., 2015) are then used as inputs to the radiative transfer calculation. The adoption of dEdd-AD radiative transfer algorithm in SNICAR, and the implementation of SNICAR snow SSPs in dEdd-AD enables a consistent simulation of the radiative effects of light-absorbing particles in the cryosphere across ESM components."

7. In the caption for Figure 1, I think you should spell out SWNB2. You refer to Figure 1 in the text before you define the acronym.
Reply: Thank you for pointing out this error. We have modified the text in Section 4 such that the original Figure 1 is not referred until SWNB2 is properly defined in the text. Note that we have switched the order of original Figures 1 and 2 since the Figure 2 in previous manuscript was the first figure cited in the text.

8. Figures 3-5 feel like they have a bunch of empty space (light red). You could almost cut off the panel axes below angles of 50 degrees.
Reply: We would agree with the Reviewer if Figures 7-8 were not included in this paper. Figures 7-8 show the errors in reflected shortwave flux given albedo errors shown in Figures 3-4, while the errors in reflected flux varies with solar zenith angles. We prefer to keep the axes of Figures 3-5 as is since it is more straightforward for cross-comparison.

9. The caption for Figure 4 is not grammatically correct and should be expanded.
Reply: Thank you for pointing this out. We have revised and expanded the figure caption.
"Figure 4. The difference in direct snow albedo ($\delta\alpha = \alpha_2 - \alpha_{16}$) computed using two-stream models (α_2) and using 16-stream DISORT model (α_{16}), for various snow depths and solar zenith angles, with snow grain radius of 1000 μm."

10. The caption for Figure 5 is not correct. These panels are not the same as Figure 3. This caption should be expanded appropriately.
Reply: Thank you for pointing this out. We have revised and expanded the figure caption.
"Figure 5. The difference in direct snow albedo ($\delta\alpha = \alpha_2 - \alpha_{16}$) computed using two-stream models (α_2) and using 16-stream DISORT model (α_{16}), for various snow depths and snow grain radii, with solar zenith angle of 60°."

11. The caption for Figure 6 is not grammatically correct and should be expanded.
Reply: Thank you for pointing this out. We have revised and expanded the figure caption.
"Figure 6. The difference in diffuse snow albedo ($\delta\alpha = \alpha_2 - \alpha_{16}$) computed using two-stream models (α_2) and using 16-stream DISORT model (α_{16}), for various snow depths and snow grain radii, with solar zenith angle of 60° at the top of the atmosphere."

12. In general, I would prefer "two-stream" rather than "2-stream".

Reply: We agree. We have replaced 2-stream with two-stream in the manuscript. Thank you for this suggestion.

Inter-comparison and improvement of two-stream shortwave radiative transfer models in ESMs for a unified treatment of cryospheric surfaces

Cheng Dang[1], Charles S. Zender[1], Mark G. Flanner[2]

[1] Department of Earth System Science, University of California, Irvine, CA, USA
[2] Department of Climate and Space Sciences and Engineering, University of Michigan, Ann Arbor, MI, USA

Correspondence to: Cheng Dang (cdang5@uci.edu)

Abstract. Snow is an important climate regulator because it greatly increases the surface albedo of large parts of the Earth. Earth System Models (ESMs) often adopt two-stream approximations with different radiative transfer techniques, the same snow therefore has different solar radiative properties depending whether it is on land or on sea ice. Here we inter-compare three two-stream algorithms widely used in snow models, improve their predictions at large zenith angles, and introduce a hybrid model suitable for all cryospheric surfaces in ESMs. The algorithms are those employed by the SNow ICe and Aerosol Radiative (SNICAR) module used in land models, and by dEdd-AD used in Icepack, the column physics used in the Los Alamos sea ice model CICE and MPAS-seaice, and a two-stream discrete ordinate (2SD) model. Compared with a 16-stream benchmark model, the errors in snow visible albedo for a direct-incident beam from all three two-stream models are small (<±0.005) and increase as snow shallows, especially for aged snow. The errors in direct near-infrared (near-IR) albedo are small (<±0.005) for solar zenith angles θ < 75°, and increase as θ increases. For diffuse incidence under cloudy skies, dEdd-AD produces the most accurate snow albedo for both visible and near-IR (<±0.0002) with the lowest underestimate (-0.01) for melting thin snow. SNICAR performs similarly to dEdd-AD for visible albedos, with a slightly larger underestimate (-0.02), while it overestimates the near-IR albedo by an order of magnitude more (up to 0.04). 2SD overestimates both visible and near-IR albedo by up to 0.03. We develop a new parameterization that adjusts the underestimated direct near-IR albedo and overestimated direct near-IR heating persistent across all two-stream models for solar zenith angles > 75°. These results are incorporated in a hybrid model SNICAR-AD, which can now serve as a unified solar radiative transfer model for snow in ESM land, land ice, and sea-ice components.

Author
Deleted: **in ESMs**

Author
Deleted: Icepack

Author
Deleted: Icepack

1. Introduction

Snow cover on land, land ice, and sea ice, modulates the surface energy balance of mid and high latitudes of the Earth, principally because even a thin layer of snow can greatly increase the surface albedo. Integrated over the solar spectrum, the broadband albedo of opaque snow ranges from 0.7 – 0.9 (e.g., Wiscombe and Warren 1980; Dang et al., 2015). In contrast, the albedo of other natural surfaces is smaller: 0.2, 0.25, and 0.5-0.7 for damp soil, grassland, and bare multi-year sea ice, respectively (Perovich 1996; Liang et al., 2002; Brandt et al., 2005; Bøggild et al., 2010). The accumulation, evolution, and depletion of snow cover modify the seasonal cycle of surface albedo globally. In particular, snow over sea ice absorbs more solar energy and begins to melt in the spring, which forms melt ponds that bring the sea-ice albedo to as low as 0.15 to further accelerate ice melt (Light et al., 2008, 2015). An accurate simulation of the shortwave radiative properties of snowpack is therefore crucial for spectrally partitioning solar energy and representing snow-albedo feedbacks across the Earth system. Unfortunately, computational demands and coupling architectures often constrain representation of snowpack radiative processes in Earth System Models (ESMs, please refer to Table 1 for all acronyms used in this work) to relatively crude approximations such as two-stream methods (Wiscombe and Warren, 1980, Toon et al., 1989). In this work, we inter-compare two-stream methods widely used in snow models and then introduce a new parameterization that significantly reduces their snowpack reflectance and heating biases at large zenith angles, to produce more realistic behavior in polar regions.

Snow albedo is determined by many factors including the snow grain radius, the solar zenith angle, cloud transmittance, light-absorbing particles, and the albedo of underlying ground if snow is optically thin (Wiscombe and Warren, 1980; Warren and Wiscombe, 1980); it also varies strongly with wavelength since the ice absorption coefficient varies by 7 orders of magnitudes across the solar spectrum (Warren and Brandt, 2008). At visible wavelengths (0.2 - 0.7 μm), ice is almost non-absorptive such that the absorption of visible energy by snowpack is mostly due to the light-absorbing particles (e.g. black carbon, organic carbon, mineral dust) that were incorporated during ice nucleation in clouds, scavenged during precipitation, or slowly sedimented from the atmosphere by gravity (Warren and Wiscombe, 1980, 1985; Doherty et al., 2010, 2014, 2016; Wang et al., 2013; Dang and Hegg 2014). As snow becomes shallower, visible photons are more likely to penetrate through snowpack and get absorbed by darker underlying ground. At near-infrared (near-IR) wavelengths (0.7 – 5 μm), ice is much more absorptive that the

Author
Deleted: large parts

Author
Deleted: and

snow albedo is lower than the visible albedo. Larger ice crystals form a lower albedo surface than smaller ice crystals hence aged snowpacks absorb more solar energy. Photons incident at smaller solar zenith angles are more likely to penetrate deeper vertically and be scattered in the snowpack until being absorbed by the ice/the underlying ground/absorbing impurities, which also leads to a smaller snow albedo. To compute the reflected solar flux, spectrally resolved albedo must be weighted by the incident solar flux, which is mostly determined by solar zenith angle, cloud cover and transmittance, and column water vapor. Modeling the solar properties of snowpacks must consider the spectral signatures of these atmospheric properties.

Several parameterizations have been developed to compute the snow solar properties without solving the radiative transfer equations and some are incorporated into ESMs or regional models. Marshall and Warren (1987) and Marshall (1989) parameterized snow albedo in both visible and near-IR bands as functions of snow grain size, solar zenith angle, cloud transmittance, snow depth, underlying surface albedo, and black carbon content. Marshall and Oglesby (1994) used this in an ESM. Gardner and Sharp (2010) parameterized the all-wave snow albedo with similar inputs. This was incorporated into the regional climate model RACMO (https://www.projects.science.uu.nl/iceclimate/models/racmo.php) to simulate snow albedo in glaciered regions like Antarctica and Greenland (Munneke et al., 2011). Dang et al., (2015) compute snow albedo as functions of snow grain radius, black carbon content, and dust content for visible and near-IR bands and 14 narrower bands used in the rapid radiative transfer model (RRTM, Mlawer and Clough, 1997). Their parameterization can also be expanded to different solar zenith angles using the zenith angle parameterization developed by Marshall and Warren (1987). Aoki et al., (2011) developed a more complex model based on the offline snow albedo and a transmittance look-up table. This can be applied to multilayer snowpack to compute the snow albedo and the solar heating profiles as functions of snow grain size, black carbon and dust content, snow temperature, and snowmelt water equivalent. These parameterizations are often in the form of simplified polynomial equations, which are especially suitable to long-term ESM simulations that require less time-consuming snow representations.

Author
Deleted: and

More complex models that explicitly solve the multiple scattering radiative transfer equations have also been developed to compute snow solar properties. Flanner and Zender (2005) developed the SNow Ice and Aerosol Radiation model (SNICAR) that utilizes two-stream approximations (Wiscombe and Warren 1980; Toon et al., 1989) to predict heating and reflectance for multi-layer snowpack. They implemented SNICAR in the Community Land Model (CLM) to predict snow albedo and vertically-resolved solar absorption for snow-covered surfaces. Before SNICAR, CLM prescribed snow albedo and confined all solar absorption to the top snow layer (Flanner and Zender 2005). Over the past decades, updates and new features have been added to SNICAR to consider more processes such as black carbon/ice mixing states (Flanner et al., 2012) and snow grain shape (He et al., 2018b). Concurrent with the development of SNICAR, Briegleb and Light (2007) improved the treatment of sea-ice solar radiative calculations in Community Climate System Model (CCSM). They implemented a different two-stream scheme with delta-Eddington approximation and adding-doubling technique (hereafter, dEdd-AD) that allows CCSM to compute bare/ponded/snow-covered sea ice albedo and solar absorption profiles of multi-layer sea ice. Before these improvements, the sea-ice albedo was computed based on surface temperature, snow thickness, and sea-ice thickness using averaged sea ice and snow albedo. dEdd-AD has been adopted by the sea-ice physics library Icepack (https://github.com/CICE-Consortium/Icepack/wiki), which is used by the Los Almos Sea Ice Model CICE (Hunke et al., 2010) and Model for Prediction Across Scales Sea Ice MPAS-seaice (Turner et al., 2018). CICE itself is used in numerous global and regional models.

SNICAR and dEdd-AD solve the multiple scattering radiative transfer equations and provide much improved solar radiative representations for the cryosphere, though their separate development and implementation created an artificial divide for snow simulation. In ESMs that utilize both SNICAR and dEdd-AD, such as the Community Earth System Model (CESM, http://www.cesm.ucar.edu/) and the Energy Exscale Earth System Model (E3SM, previously known as ACME, https://e3sm.org/), the solar radiative properties of snow on land and snow on sea ice are computed separately via SNICAR and dEdd-AD. As a result, the same snow in nature has different solar radiative properties such as reflectance depending on which model represents it. These differences are model artifacts that should be eliminated so that snow has consistent properties across the Earth system.

In this paper, we evaluate the accuracy and biases of three two-stream models listed in Table 2, including the algorithms used in SNICAR and dEdd-AD, at representing reflectance and heating. In Sections 2-4, we describe the radiative transfer algorithms and calculations performed in this work. The results and model inter-comparisons are discussed in Section 5. In Section 6, we introduce a parameterization to reduce the

Author
Deleted: two-stream delta-Eddington method

Author
Deleted: that

Author
Deleted: This method has carried into

Author
Deleted:

Author
Deleted: that

Author
Deleted: comprises the column physics

Author
Deleted: .

Author
Deleted: The shortwave methods in SNICAR and in CICE

Author
Deleted: CICE/MPAS-seaice

Author
Deleted: CICE/MPAS-seaice

Author
Deleted: algorithms

Author
Deleted: described

Author
Deleted: in Section 2 and

Author
Deleted: 1

Author
Deleted: Icepack

simulated albedo and heating bias for solar zenith angles larger than 75°. In Section 7, we summarize the major differences of algorithm implementations between SNICAR and dEdd-AD in ESMs. We use these results to develop and justify a unified surface shortwave radiative transfer method for all Earth system model components in the cryosphere, presented in Section 8.

Author
Deleted: .

2. Radiative Transfer Model

In this section, we summarize the three two-stream models and the benchmark DISORT model with 16-streams. These algorithms are well documented in papers by Toon et al., (1989), Briegleb and Light (2007), Jin and Stamnes (1994), and Stamnes et al. (1988). Readers interested in detailed mathematical derivations should refer to those papers. We only include their key equations to illustrate the difference among two-stream models for discussion purposes.

2.1 SNICAR in land models CLM and ELM

SNICAR is implemented as the default snow shortwave radiative transfer scheme in CLM and E3SM land model (ELM). It adopts the two-stream algorithms and the rapid solver developed by Toon et al., (1989) to compute the solar properties of multi-layer snowpacks. These two-stream algorithms are derived from the general equation of radiative transfer in a plane parallel media:

$$\mu \frac{\partial I}{\partial \tau}(\tau, \mu, \Phi) = I(\tau, \mu, \Phi) - \frac{\varpi}{4\pi} \int_0^{2\pi} \int_{-1}^{1} P(\mu, \mu', \phi, \phi')\, I(\tau, \mu', \Phi') d\mu' d\phi' - S(\tau, \mu, \Phi) \quad (1)$$

where arccos(μ) and Φ are zenith angle and azimuth angle, ϖ is single-scattering albedo. On the right-hand side, the three terms are intensity at optical depth τ, internal source term due to multiple scattering, and external source term S. For a purely external source at solar wavelengths S is:

$$S = \frac{\varpi}{4} F_s P(\mu, -\mu_0, \phi, \phi_0) exp\,(\frac{-\tau}{\mu_0}) \quad (2)$$

where πF_s is incident solar flux, μ_0 is the incident direction of the solar beam. Integrating equation (1) over azimuth and zenith angles yields the general solution of two-stream approximations (Meador and Weaver, 1980). The upward and downward fluxes at optical depth τ of layer n can be represented as:

$$F_n^+ = k_{1n}\, exp(\Lambda_n \tau) + \Gamma_n k_{2n}\, exp(-\Lambda_n \tau) + C_n^+(\tau) \quad (3a)$$

$$F_n^- = \Gamma_n k_{1n}\, exp(\Lambda_n \tau) + k_{2n}\, exp(-\Lambda_n \tau) + C_n^-(\tau) \quad (3b)$$

where Λ_n, Γ_n C_n are known coefficients determined by the two-stream method, incident solar flux, and solar zenith angle; whereas k_{1n} and k_{2n} are unknown coefficients determined by the boundary conditions. For an N-layer snowpack, the solutions for upward and downward fluxes are coupled at layer interfaces to generate 2N equations with 2N unknown coefficients k_{1n} and k_{2n}. Combining these equations linearly generates a new set of equations with terms in tridiagonal form that enables the application of a fast tri-diagonal matrix solver. With the solved coefficients, the upward and downward fluxes are computed at different optical depths (Equations 3a and 3b) and eventually the reflectance, transmittance, and absorption profiles of solar flux for any multilayer snowpack.

SNICAR itself implements all three two-stream algorithms in Toon et al., (1989): Eddington, Quadrature, and Hemispheric-mean. In practical simulations, it utilizes the Eddington and Hemispheric-mean approximations to compute the visible and near-IR snow properties, respectively (Flanner et al., 2007). In addition to their algorithms, SNICAR implements the Delta-transform of the fundamental input variables asymmetry factor (g), single-scattering albedo (ϖ), and optical depth (τ) to account for the strong forward scattering in snow (Equations 2 (a)-(c), Wiscombe and Warren, 1980).

2.2. dEdd-AD in sea ice models Icepack, CICE, and MPAS-seaice

Icepack, CICE, and MPAS-seaice use the same shortwave radiative scheme dEdd-AD developed and documented by Briegleb and Light (2007). Sea ice is divided into multiple layers to first compute the single-layer reflectance and transmittance using two-stream delta-Eddington solutions to account for the multiple scattering of light within each layer (Equation set 50, Briegleb and Light, 2007), where the name "delta" implies dEdd-AD implements the Delta-transform to account for the strong forward scattering of snow and

Author
Deleted: solar

Author
Deleted: treatment

Author
Deleted: In the following discussions, we will refer to this method as CICE since it is more widely used.

Author
Deleted:), where

Author
Deleted: the

Author
Deleted: CICE

sea ice (Equations 2 (a)-(c), Wiscombe and Warren, 1980). The single-layer direct albedo and transmittance are computed by equations:

$$R(\mu_{0,n}) = A_n\, exp\left(\frac{-\tau}{\mu_{0,n}}\right) + B_n(exp(\varepsilon_n\tau) - exp(-\varepsilon_n\tau)) - K_n \quad (4a)$$

$$T(\mu_{0,n}) = E_n + H_n(exp(\varepsilon_n\tau) - exp(-\varepsilon_n\tau))\, exp\left(\frac{-\tau}{\mu_{0,n}}\right) \quad (4b)$$

where coefficients A_n, B_n, K_n, E_n, H_n, and ε_n are determined by the single-scattering albedo (ϖ), asymmetry factor (g), optical depth (τ), and angle of the incident beam at layer n ($\mu_{0,n}$). Following the delta-Eddington assumption, simple formulas are available for the single-layer reflectance and transmittance under both clear sky (direct flux, equations 4a and 4b) and overcast sky (diffuse flux) conditions, however, the formula derived by applying diffuse-flux upper boundary conditions sometimes yields negative albedos (Wiscombe 1977). To avoid the unphysical values, diffuse reflectance $\bar{R}$and transmittance $\bar{T}$ of a single layer are computed by integrating the direct reflectance $R(\mu)$ and transmittance $T(\mu)$ over the incident hemisphere assuming isotropic incidence:

$$\bar{R} = 2\int_0^1 \mu R(\mu) d\,\mu \quad (5a)$$

$$\bar{T} = 2\int_0^1 \mu T(\mu) d\,\mu \quad (5b)$$

This is the same as the method proposed by Wiscombe and Warren (1980, their equation 5). In practice, eight Gaussian angles are implemented to perform the integration for every layer.

The computed single-layer reflectance and transmittance of direct and diffuse components are then combined to account for the inter-layer scattering of light to compute the reflectance and transmission at every interface (Equation set 51, Briegleb and Light, 2007), and eventually the upward and downward fluxes (Equation set 52, Briegleb and Light, 2007). These upward and downward fluxes at each optical depth are then used to compute the column reflectance and transmittance, and the absorption profiles for any multilayered media, such as snowpacks on land and sea ice.

In nature, a large fraction of sea ice is covered by snow during winter. As snow melts away in late spring and summer, it exposes bare ice, and melt ponds form on the ice

Author
Deleted: se

surface. Such variation of sea-ice surface types requires the shortwave radiative transfer model to be flexible and capable of capturing the light refraction and reflection. Refractive boundaries exist where air (refractive index m_{re} = 1.0), snow (assuming snow as medium of air containing a collection of ice particles, m_{re} = 1.0), pond (assuming pure water, m_{re} = 1.33), and ice (assuming pure ice, m_{re} = 1.31) are present in the same sea-ice column. The general solution of delta-Eddington, and the two-stream algorithms used in SNICAR are not applicable to such non-uniformly refractive layered media. To include the effects of refraction, Briegleb and Light (2007) modified the adding formula at the refractive boundaries (i.e. interfaces between air/ice, snow/ice, air/pond). The reflectance and transmittance of the adjacent layers above and below the refractive boundary are combined with modifications to include the Fresnel reflection and refraction of direct and diffuse fluxes (Section 4.1, Briegleb and Light, 2007). dEdd-AD can thus be applied to any layered media with either uniform (e.g., snow on land) or non-uniform (e.g., snow on sea ice) refractive indexes.

In this paper, we apply dEdd-AD to snowpacks that can be treated as uniform refractive media such as the air/snowpack/land columns assumed in SNICAR for model evaluation. An ideal radiative treatment for snow should, however, keep the potential to include refraction for further applications to snow on sea ice or ice sheets. Therefore, besides these two widely used algorithms in Icepack and SNICAR, we evaluate a third algorithm (section 2.3) that can be applied to layered media with either uniform or non-uniform refractive indexes.

2.3. two-stream discrete-ordinate algorithm (2SD)

A refractive boundary also exists between the atmosphere and the ocean, and models have been developed to solve the radiative transfer problems in the atmosphere-ocean system using the discrete-ordinate technique (e.g. Jin and Stamnes, 1994; Lee and Liou, 2007). Similar to the two-stream algorithms of Toon et al., (1989) used in SNICAR, Jin and Stamnes (1994) also developed their algorithm from the general equation:

$$\mu \frac{\partial I}{\partial \tau}(\tau,\mu) = I(\tau,\mu) - \frac{\varpi}{4\pi}\int_{-1}^{1} P(\tau,\mu,\mu')\, I(\tau,\mu')\, d\mu' - S(\tau,\mu) \qquad (6)$$

Equation (6) is the azimuthally integrated version of equation (1). However, for vertically inhomogeneous media like the atmosphere-ocean or sea ice, the external source term $S(\tau,\mu)$ is different. Specifically, for the medium of total optical depth τ^{a} above the

Author
Deleted: This adding-doubling delta-Eddington method

Author
Deleted: .

Author
Deleted: focus on

refractive interface, one must consider the contribution from the upward beam reflected at the refractive boundary (second term on the right-hand side):

$$S^a(\tau,\mu) = \frac{\varpi}{4\pi} F_s P(\tau, -\mu_0, \mu)\, exp\left(\frac{-\tau}{\mu_0}\right) + \frac{\varpi}{4\pi} F_s R(-\mu_0, m) P(\tau, +\mu_0, \mu) exp\left(\frac{-(2\tau^a - \tau)}{\mu_0}\right) \tag{7}$$

where $R(-\mu_0, m)$ is the Fresnel reflectance of radiation and m is the ratio of the refractive indices of the lower to the upper medium. For the medium below the refractive interface, one must account for the Fresnel transmittance $T(-\mu_0, m)$ and modify the angle of beam travel in media b:

$$S^b(\tau,\mu) = \frac{\varpi}{4\pi}\frac{\mu_0}{\mu_{0n}} F_s T(-\mu_0, m) P(\tau, -\mu_0, \mu)\, exp\left(\frac{-\tau^a}{\mu_0}\right) exp\left(\frac{-(\tau - \tau^a)}{\mu_{0n}}\right) \tag{8}$$

where μ_{0n} is the cosine zenith angle of refracted beam incident at angle μ_0 above the refractive boundary, by Snell's law:

$$\mu_{0n} = \sqrt{1 - (1 - \mu_0^2)/m^2} \tag{9}$$

For uniformly refractive media like snow on land, one can just set the refractive index m_{re} equal to 1 for every layer. In this case, the Fresnel reflectance $R(-\mu_0, m)$ is 0 in equation (7), the Fresenal transmittance $T(-\mu_0, m)$ is 1 in equation (8), and μ_{0n} equals to μ_0: the two source terms $S^a(\tau,\mu)$ and $S^b(\tau,\mu)$ become the same and equal to the source term of homogenous media given in equation (2).

For two-stream approximations of this method, analytical solutions of upward and downward fluxes are coupled at each layer interface to generate 2N equations with 2N unknown coefficients for any N-layer stratified column. The solutions of two-stream algorithms and boundary conditions for homogenous media are well documented (Sections 8.4 and 8.10 of Thomas and Stamnes, 1999). Despite the extra source terms, these 2N equations can also be organized into a tridiagonal matrix similar to the method of Toon et al. (1989) used in SNICAR. Flexibility and speed therefore make this two-stream discrete-ordinate algorithm (hereafter, 2SD) a potentially good candidate for long-term Earth system modeling. In this work, we only apply 2SD to snowpack and note that it can be applied to any uniformly or non-uniformly refractive media like snow on land or sea ice, with the Delta-transform implemented to fundamental optical variables (Equations 2 (a)-(c), Wiscombe and Warren, 1980).

2.4 16-stream DISORT

Besides the mathematical technique, the accuracy and speed of radiative transfer algorithms depend on the number of angles used for flux estimation in the upward and downward hemispheres. SNICAR, dEdd-AD, and 2SD use one angle to represent upward flux and one angle to represent downward flux, hence they are named two-stream algorithm. Lee and Liou (2007) use two upward and two downward streams. Jin and Stamnes (1994) documented the solutions for any even number of streams. The computational efficiency of these models is lower than that of two-stream models while their accuracy is better. To quantify the accuracy of the three two-stream algorithms for snow shortwave simulations, we use the 16-stream DIScrete-Odinate Radiative Transfer model (DISORT) as the benchmark model (http://lllab.phy.stevens.edu/disort/) (Stamnes et al., 1988).

3. Input for radiative transfer models

In this work, we focus on the performance of two-stream algorithms for pure snow simulations. The inputs for these three models are the same: single-scattering properties (SSPs, i.e. single-scattering albedo ϖ, asymmetry factor g, extinction coefficient σ_{ext}) of snow determined by snow grain radius r, snow depth, solar zenith angle θ, solar incident flux, and the albedo of underlying ground (assuming Lambertian reflectance of 0.25 for all wavelengths). A Delta-transform is applied to fundamental input optical variables for all simulations (Equations 2 (a)-(c), Wiscombe and Warren, 1980).

In snow, photon scattering occurs at the air-ice interface, and the absorption of photons occurs within the ice crystal. The most important factor that determines snow shortwave properties is the ratio of total surface area to total mass of snow grains, aka "the specific surface area" (e.g. Matzl and Schneebeli, 2006, 2010). The specific surface area (β) can be converted to a radiatively effective snow grain radius r:

$$\beta = 3 / (r \rho_{ice}) \quad (10)$$

Author
Deleted: The algorithms used in

Author
Deleted: Icepack

Author
Deleted: speed

Author
Deleted: slower

where ρ_{ice} is the density of pure ice, 917 kg m^{-3}. Assuming the grains are spherical, the SSPs of snow can thus be computed using Mie theory (Wiscombe, 1980) and ice optical constants (Warren and Brandt, 2008). In nature, snow grains are not spherical, and many studies have been carried out to quantify the accuracy of such spherical representations (Grenfell and Warren, 1999; Neshyba et al., 2003; Grenfell et al., 2005). In recent years, more research has been done to evaluate the impact of grain shape on snow shortwave properties (Dang et al., 2016; He et al., 2017, 2018ab), and they show that non-spherical snow grain shapes mainly alter the asymmetry factor. Dang et al., (2016) also point out that the solar properties of a snowpack consisting of non-spherical ice grains can be mimicked by a snowpack consisting of spherical grains with a smaller grain size by factors up to 2.4. In this work, we still assume the snow grains are spherical, and this assumption does not qualitatively alter our evaluation of the radiative transfer algorithms.

The input SSPs of snow grains are computed using Mie theory at a fine spectral resolution for a wide range of ice effective radius *r* from 10 to 3000 μm that covers the possible range of grain radius for snow on Earth (Flanner et al., 2007). The same spectral SSPs were also used to derive the band-averaged SSPs of snow used in SNICAR. Note Briegleb and Light (2007) refer to SSPs as inherent optical properties.

4. Solar spectra used for the spectral integrations

In climate modeling, snow albedo computation at a fine spectral resolution is expensive and unnecessary. Instead of computing spectrally resolved snow albedo as shown in Figure 1, wider-band solar properties are more practical. For example, CESM and E3SM aggregate the narrow RRTMG bands used for the atmospheric radiative transfer simulation into visible (0.2 - 0.7 μm) and near-IR (0.7 - 5 μm) bands. The land model and sea-ice model thus receive visible and near-IR fluxes as the upper boundary condition, and return the corresponding visible and near-IR albedos to atmosphere model. In practice, these bands are also partitioned into direct and diffuse components. Therefore, a practical two-stream algorithm should be able to simulate the direct visible, diffuse visible, direct near-IR and diffuse near-IR albedos and absorptions of snow accurately.

The band albedo α is an irradiance-weighted average of the spectral albedo $\alpha(\lambda)$:

$$\alpha = \frac{\int_{\lambda 1}^{\lambda 2} \alpha(\lambda) F(\lambda) d\lambda}{\int_{\lambda 1}^{\lambda 2} F(\lambda) d\lambda} \tag{11}$$

In this work, we use the spectral irradiance $F(\lambda)$ generated by the atmospheric DISORT-based Shortwave Narrowband Model (SWNB2) (Zender et al., 1997; Zender, 1999) for typical clear-sky and cloudy-sky conditions of mid-latitude winter as shown in Figure 2(a). The total clear-sky down-welling surface flux at different solar zenith angles are also given in Figure 2(b).

5. Model Evaluation

5.1 Spectral albedo and reflected solar flux

The spectral reflectance of pure deep snow computed using two-stream models and 16-stream DISORT are shown in Figure 1. The snow grain radius is 100 µm - a typical grain size for fresh new snow. For clear sky with direct beam source (left column), all three two-stream models show good accuracy at visible wavelengths (0.3 – 0.7 µm), and within this band, the snow albedo is large and close to 1. As wavelength increases, the albedo diminishes in the near-IR band. two-stream models overestimate snow albedo at these wavelengths, with maximum biases of 0.013 (SNICAR and dEdd-AD) and 0.023 (2SD) within wavelength 1 - 1.7 µm. For cloudy-sky cases with diffuse upper boundary conditions, dEdd-AD reproduces the snow albedo at all wavelengths with the smallest absolute error (< 0.005), SNICAR and 2SD both overestimate the snow albedo with maximum biases > 0.04 between 1.1-1.4 µm.

In both sky conditions, the errors of snow albedo are larger at near-IR wavelengths ranging from 1.0-1.7 µm, while the solar incident flux peaks at 0.5 µm then decrease as wavelength increases. The largest error in reflected flux is within the 0.7-1.5 µm band for SNICAR and 2SD, as shown in the 3rd row of Figure 1. dEdd-AD overestimate the direct snow albedo mostly at wavelengths larger than 1.5 µm where the error in reflected flux is almost negligible.

5.2 Broadband albedo and reflected solar flux

Integrated over the visible and near-IR wavelengths, the error in band albedos computed using two-stream models for different cases are shown in Figure 3-6.

Figure 3 shows the error in direct band albedo for fixed snow grain radius of 100 µm with different snow depth and solar zenith angles. As introduced in Section 2, SNICAR and dEdd-AD both use delta-Eddington method to compute the visible albedo. They overestimate the visible albedo for solar zenith angles smaller than 50° by up to 0.005,

Author
Deleted: Figure 2

Author
Deleted: CICE

Author
Deleted: CICE

Author
Deleted: s

Author
Deleted: Figure 2

Author
Deleted: CICE

Author
Deleted: CICE

and underestimate it for solar zenith angles larger than 50° by up to -0.01. 2SD produces similar results for the visible band but at a larger solar zenith angle threshold of 75°. In the near-IR band, SNICAR and 2SD overestimate the snow albedo for solar zenith angles smaller than 70°, beyond this, the error in albedo increases by up to -0.1 as solar zenith angle increases. dEdd-AD produces a similar error pattern with a smaller solar zenith angle threshold at 60°. As snow ages, its average grain size increases. For typical old melting snow of grain radius 1000 μm (Figure 4), two-stream models produce similar errors of direct albedo in all bands. For snow consisting of smaller grain size, two-stream models produce larger errors for visible albedo. Integrating over the entire solar band, the three two-stream models evaluated show similar error patterns for direct albedo.

For a fixed solar zenith angle of 60°, the error of direct albedo for different snow depth and snow grain radii are shown in Figure 5. SNICAR and dEdd-AD underestimate the visible albedo in most scenarios, while 2SD overestimates the visible albedo for a larger range of grain radius and snow depth. All three two-stream models tend to overestimate the near-IR albedo except for shallow snow with large grain radius; the error of 2SD is one order of magnitude larger than that of SNICAR and dEdd-AD.

Figure 6 is similar to Figure 5, but shows the diffuse snow albedo. In the visible band, SNICAR and dEdd-AD generate similar errors in that they both underestimate the albedo as snow grain size increases and snow depth decreases. 2SD overestimates the albedo with a maximum error of around 0.015. In the near-IR, two-stream models tend to overestimate snow albedo, while the magnitude of biases produced by SNICAR and 2SD are one order larger than that of dEdd-AD with the maximum error of 0.035 generated by SNICAR. As a result, the all-wave diffuse albedos computed using dEdd-AD are more accurate than those computed using SNICAR and 2SD.

Figures 7, 8 and 9 show the errors in reflected shortwave flux caused by snow albedo errors seen in Figures 3, 4, and 6. In general, two-stream models produce larger errors in reflected direct near-IR flux (Figure 7 and 8), especially with the 2SD model: the maximum overestimate of reflected near-IR flux is 6-8 Wm^{-2} for deep melting snow with solar zenith angle < 30°. Errors in reflected direct visible flux are smaller (mostly within ±1 Wm^{-2})for all models in most scenarios, and become larger (mostly within ±3 Wm^{-2}) as snow grain size increases to 1000 μm if computed using 2SD. As shown in Figure 9, for diffuse flux with solar zenith angle of 60° at TOA, SNICAR and dEdd-AD generate

Author
Deleted: CICE

Author
Deleted: CICE

Author
Deleted: CICE

Author
Deleted: CICE

Author
Deleted: CICE

Author
Deleted: CICE

Author
Deleted: CICE

small errors in reflected visible flux (mostly within ±1 Wm^{-2}), while 2SD always overestimates reflected visible flux by up to 5 Wm^{-2}. In the near-IR, SNICAR and 2SD overestimate reflected flux by as much as 10-12 Wm^{-2}; the error in reflected near-IR flux produced by dEdd-AD is much smaller, mostly within ±1 Wm^{-2}.

In general, dEdd-AD produces the most accurate albedo and thus reflected flux for both direct and diffuse components. SNICAR is similar to dEdd-AD for its accuracy of direct albedo and flux, yet generates large error for the diffuse component. 2SD tends to overestimate snow albedo and reflected flux in both direct and diffuse components and shows the largest errors among three two-stream models. These relatively small differences between algorithms may still yield large impact on snowpack. For example, compared to dEdd-AD, SNICAR and 2SD overestimate the diffuse albedo by ~0.015 for melting snow (Figure 6). In Greenland, the daily averaged downward diffuse solar flux from May to September is 200 W/m^2, and the averaged cloud cover fraction is 80% (Figure 6, Dang et al., 2017). In this case, SNICAR and 2SD overestimate the reflected solar flux by 2.4 W/m^2 per day – the amount of energy otherwise enough to melt 10 cm of snow water equivalent from May to September. dEdd-AD also remediates self-compensating spectral biases (where visible and Near-IR biases are of opposite signs) present in the other schemes. Those spectral biases do not affect the broadband fluxes like the diffuse biases, but they nevertheless degrade proper feedbacks between snow/ice reflectance and heating."

5.3 Band absorption of solar flux

Figure 10 shows absorption profiles of shortwave flux computed using the 16-stream DISORT model, with errors in absorbed fractional solar flux computed using two-stream models. The snowpack is 10-cm deep and is divided into 5 layers, each 2-cm thick. The snow grain radius is set to 100 μm. The figure shows fractional absorption for snow layers 1-4 and the underlying ground with an albedo of 0.25.

As shown in the first column of Figure 10, for new snow with a radius of 100 μm, most solar absorption occurs in the top 2-cm snow layer, where roughly 10% and 15% of diffuse and direct near-IR flux are absorbed and dominate the solar absorption within the snowpack. In the second layer (2-4 cm), the absorption of solar flux is less than 1% and gradually decreases within the interior layers. The underlying ground absorbs roughly 2% of solar flux, mostly visible flux that penetrates the snowpack more efficiently. As snow

Author
Deleted: CICE

Author
Deleted: CICE

Author
Deleted: CICE

Author
Deleted: Note that the final errors of snow albedo and reflected solar flux are the weighted sum of direct and diffuse components, and their weights are largely determined by cloud cover fraction (e.g. Figure 6, Dang et al., 2017), which we do not address explicitly in this paper.

Author
Deleted: ,

Author
Deleted:

ages and snow grain grows, photons penetrate deeper into the snowpack. For typical old melting snow with a radius of 1000 μm, most solar absorption still occurs in the top 2-cm snow layer, where roughly 20% and 14% of diffuse and direct near-IR flux are absorbed. The second snow layer (2-4 cm) absorbs more near-IR solar flux by roughly 2%. More photons can penetrate through the snowpack, and results in a high fractionally absorption by the underlying ground, especially for the visible band. As snow depth increase, the ground absorption will decrease for both snow radii.

Author
Deleted: are able to

Comparing to 16-stream DISORT, two-stream models underestimate (overestimate) the column solar absorptions for new (old) snow, especially for the surface snow layer and the underground. Overall, dEdd-AD gives the most accurate absorption profiles among the three two-stream models, especially for new snow.

Author
Deleted: layer.

Author
Deleted: CICE

6. Correction for direct albedo for large solar zenith angles

It has been pointed out in previous studies that the two-stream approximations become poor as solar zenith angle approaches 90° (e.g. Wiscombe 1977, Warren 1982). As shown in Figures 3 and 4, all three two-stream models underestimate the direct snow albedo for large solar zenith angles. In the visible band, when the snow grain size is small, the error in direct albedo is almost negligible (Figure 3); while as snow ages and snow grains become larger, the error increases yet remains low if the snow is deep (Figure 4). In the near-IR, the biases of albedo are also larger for larger snow grain radii. For a given snow size, the magnitudes of such biases are almost independent of snow depth, and mainly determined by the solar zenith angle. In general, the errors of all-wave direct albedo are mostly contributed by the errors of near-IR albedo, especially for optically thick snowpacks (i.e., semi-infinite), because the errors of direct albedo in the visible are negligible compared with those in the near-IR. To improve the performance of two-stream algorithms, we develop a parameterization that corrects the underestimated near-IR snow albedo at large zenith angles.

Author
Deleted: 1997

Author
Deleted: still

Figure 11 shows the direct near-IR albedo and fractional absorption of 2-meter thick snowpacks consisting of grains with radius 100 μm and 1000 μm, computed using two-stream algorithms and 16-stream DISORT. For solar zenith angles > 75°, two-stream models underestimate snow albedo and overestimate solar absorption within snowpack, mostly in the top 2-cm of snow, and the differences among three two-stream models are small. In Section 5, we have shown that dEdd-AD produces the most accurate snow

Author
Deleted: a

albedo in general, with anticipated wide application of dEdd-AD, we develop the following parameterization to adjust its low biases in computed near-IR direct albedo.

We define and compute R_{75+} as the ratio of direct semi-infinite near-IR albedo computed using 16-stream DISORT ($\alpha_{16\text{-}DISORT}$) to that computed using dEdd-AD ($\alpha_{dEdd\text{-}AD}$). This ratio is shown in Figure 11 (c) and can be parameterized as a function of snow grain radius (r, unit in meter) and the cosine of incident solar zenith angle (μ_0), as shown in Figure 11(c):

$$R_{75+} = \frac{\alpha_{16-DISORT}}{\alpha_{dEdd-AD}} = c_1(\mu_0)log_{10}(r) + c_0(\mu_0) \quad (12)$$

where coefficients c_1 and c_0 are polynomial functions of μ_0, as shown in Figure 11(d):

$$c_1(\mu_0) = 1.304\mu_0^2 - 0.631\mu_0 + 0.086 \quad (13a)$$

$$c_0(\mu_0) = 6.807\mu_0^2 - 3.338\mu_0 + 1.467 \quad (13b)$$

Since two-stream models always underestimate snow albedo, R_{75+} always exceeds 1 (Figure 11c). We can then adjust the direct near-IR snow albedo ($\alpha_{dEdd\text{-}AD}$) and direct near-IR solar absorption ($Fabs_{dEdd\text{-}AD}$) by snow computed using dEdd-AD with ratio R_{75+}:

$$\alpha_{dEdd-AD}^{adjust} = R_{75+}\alpha_{dEdd-AD} \quad (14a)$$

$$Fabs_{dEdd-AD}^{adjust} = Fabs_{dEdd-AD} - (R_{75+} - 1)\alpha_{dEdd-AD}F_{nir} \quad (14b)$$

where F_{nir} is the direct near-IR flux. This adjustment reduces the error of near-IR albedo from negative 2-10% to within ± 0.5% for solar zenith angles larger than 75°, and for grain radii ranging from 30-1500 µm (Figure 12). Errors in broadband direct albedo are therefore also reduced to < 0.01. The direct near-IR flux absorbed by the snowpack decreases after applying this adjustment.

When the solar zenith angle exceeds 75°, our model adjusts the computed direct near-IR albedo αdEdd-AD by the ratio *R75+* following equations 12-14a and reduces direct near-

Author
Deleted: CICE
Author
Deleted: CICE
Author
Deleted: CICE
Author
Deleted: CICE
Author
Deleted: CICE
Author
Deleted: CICE
Author
Deleted: R75
Author
Author
Deleted: CICE
Author
Deleted:
Author
Author
Deleted: CICE
Author
Deleted: *
Author
Deleted: CICE*
Author
Deleted: *
Author
Formatted: None, Font:(Default) Times
Author
Formatted: None, Font:(Default) Cambria
Author
Formatted: None, Font:(Default) Times, Subscript
Author
Formatted: None, Font:(Default) Times
Author
Formatted ... [1]
Author
Formatted: Subscript
Author
Formatted: None, Font:(Default) Times
Author
Formatted: None, Font:(Default) Times

IR absorption following equation 14b. If snow is divided into multiple layers, we assume all decreased near-IR absorption (2^{nd} term on the right-hand side, equation 14b) is confined within the top layer. This assumption is fairly accurate for the near-IR band, since most absorption occurs at the surface of snowpack (Figures 10 and 11). As discussed previously, this parameterization is developed based on albedo computed using dEdd-AD. For models that do not use dEdd-AD but SNICAR and 2SD, the same adjustment still applies given the small differences of near-IR direct albedo computed using two-stream models (Figure 11). For models that adopt other radiative transfer algorithms it is best for the developers to examine their model against a benchmark model such as 16-stream DISORT or two-stream models discussed in this work before applying this correction.

Author
Deleted: In practice,

Author
Deleted: if

Author
Deleted: right

Author
Deleted: direct IR

It is important to note that although the errors of direct near-IR albedos are large for large solar zenith angles, the absolute error in reflected shortwave flux is small (Figures 7 and 8) as the down-welling solar flux reaches snowpack decreases as solar zenith angle increases (Figures 1(b)). However, such small biases in flux can be important to high latitudes where the solar zenith angle remains large for many days in late winter and early spring.

Author
Deleted: at

Author
Deleted: We have implemented this parameterization in MPAS-seaice to quantify its impact on polar climate, though these experiments are beyond the scope of the present paper.

7. Implementation of snow radiative transfer model in Earth system models

ESMs often use broader band-averaged SSPs of snow and aerosols for computational efficiency, rather than using brute-force integration of spectral solar properties across narrower bands (per equation 11). Besides using different radiative transfer approximations, SNICAR and dEdd-AD also adopt different methods to derive the band-averaged SSPs of snow for different band schemes.

Author
Deleted: CICE

In SNICAR, snow solar properties are computed for 5 bands: one visible band (0.3 - 0.7μm), and four near-IR bands (0.7 - 1 μm, 1 – 1.2 μm, 1.2 – 1.5 μm, and 1.5 – 5 μm). The solar properties of four subdivided near-IR bands are combined by fixed ratios to compute the direct/diffuse near-IR snow properties. These two sets of ratios are derived offline based on the incident solar spectra of typical of mid-latitude winter for clear and cloudy-sky conditions clear sky and cloudy sky, respectively (Figure 1(a)).

The band-averaged SSPs of snow grains are computed following the Chandrasekhar Mean approach (Thomas and Stamnes, 1999, their Equation 9.27; Flanner et al., 2007).

Specifically, spectral SSPs of snow grains are weighted into bands according to surface incident solar flux typical of mid-latitude winter for clear and cloudy sky conditions. In addition, the single-scattering albedo $\varpi(\lambda)$ of ice grains are also weighted by the hemispheric albedo $\alpha(\lambda)$ of an optically thick snowpack:

$$\varpi(\bar{\lambda}) = \frac{\int_{\lambda_1}^{\lambda_2} \varpi(\lambda)F(\lambda)\alpha(\lambda)d\lambda}{\int_{\lambda_1}^{\lambda_2} F(\lambda)\alpha(\lambda)d\lambda} \quad (15a)$$

$$g(\bar{\lambda}) = \frac{\int_{\lambda_1}^{\lambda_2} g(\lambda)F(\lambda)d\lambda}{\int_{\lambda_1}^{\lambda_2} F(\lambda)\alpha(\lambda)d\lambda} \quad (15b)$$

$$\sigma_{ext}(\bar{\lambda}) = \frac{\int_{\lambda_1}^{\lambda_2} \sigma_{ext}(\lambda)F(\lambda)d\lambda}{\int_{\lambda_1}^{\lambda_2} F(\lambda)\alpha(\lambda)d\lambda} \quad (15c)$$

Two sets of snow band-averaged SSPs are generated for all grain radii, suitable for direct and diffuse light, respectively. For each modeling step and band, SNICAR is called twice to compute the direct and diffuse snow solar properties.

In dEdd-AD, the snow-covered sea ice properties are computed for 3 bands: one visible band (0.3 – 07 µm), and two near-IR bands (0.7 – 1.19 µm and 1.19 – 5 µm). The solar proprieties of these two near-IR bands are combined using ratios w_{nir1} and w_{nir2} for 0.7-1 .19 µm and 1.19-5 µm, depending on the fraction of direct near-IR flux f_{nidr}:

$$w_{nir1} = 0.67 + 0.11 * (1 - f_{nidr}) \quad (16a)$$

$$w_{nir2} = 1 - w_{nir1} \quad (16b)$$

The band SSPs of snow are derived by integrating the spectral SSPs and the spectral surface solar irradiance measured in the Arctic under mostly clear sky.

$$\varpi(\bar{\lambda}) = \int_{\lambda_1}^{\lambda_2} \varpi(\lambda)F(\lambda)d\lambda \quad (17a)$$

$$g(\bar{\lambda}) = \int_{\lambda_1}^{\lambda_2} g(\lambda)F(\lambda)d\lambda \quad (17b)$$

$$\sigma_{ext}(\bar{\lambda}) = \int_{\lambda_1}^{\lambda_2} \sigma_{ext}(\lambda)F(\lambda)d\lambda \quad (17c)$$

Author
Deleted: CICE

In addition, the band-averaged single-scattering albedo $\varpi(\bar{\lambda})$ is also increased to $\varpi(\bar{\lambda})'$ until the band albedo computed using averaged SSPs matches the band albedo $\bar{\alpha}$ within 0.0001, where $\bar{\alpha}$ is:

$$\bar{\alpha} = \int_{\lambda_1}^{\lambda_2} \alpha(\lambda)F(\lambda)d\lambda \quad (18)$$

dEdd-AD adopts this single set of band SSPs for both direct and diffuse computations. In practice, the physical snow grain radius r is adjusted to a radiatively equivalent radius r_{eqv} based on the fraction of direct flux in the near-IR band (f_{nidr}):

$$r_{eqv} = (f_{nidr} + 0.8(1 - f_{nidr}))r \quad (19)$$

This r_{eqv} and the corresponding snow SSPs are then used in the radiative transfer calculation. The computed direct and diffuse solar properties alone are less accurate, while the combined all-sky broadband solar properties agree with SNICAR (Briegleb and Light, 2007). As a result, for each modeling step and band, dEdd-AD radiative transfer subroutine is called only once to compute both the direct and diffuse snow solar properties simultaneously.

SNICAR and dEdd-AD also use different approaches to avoid numerical singularities. In SNICAR, singularities occur when the denominator of term $C_n^{\pm}$ in equation (3) equals to zero (i.e., $\gamma^2 - 1/\mu_0^2 = 0$), where γ is determined by the approximation method and SSPs of snow, and μ_0 is the cosine of the solar zenith angle (Equations 23 and 24, Toon et al., 1989). When such a singularity is detected, SNICAR will shift μ_0 by + 0.02 or -0.02 to obtain physically realistic radiative properties. In the dEdd-AD algorithm, singularities arise only when μ_0= 0 (Equation 4). Therefore, in practice, for $\mu_0 < 0.01$, dEdd-AD computes the sea-ice solar properties for $\mu_0 = 0.01$ to avoid unphysical results.

8. Discussion: a unified radiative transfer model for snow, sea ice, and land ice.

Based on the inter-comparison of three two-stream algorithms and their implementations in ESMs, we formulated the following surface shortwave radiative transfer

Author
Deleted: CICE

Author
Deleted: CICE

Author
Deleted: CICE

Author
Deleted: CICE

Author
Deleted: CICE

recommendations for an accurate, fast, and consistent treatment for snow on land, land ice, and sea ice in ESMs:

First, the two-stream delta-Eddington adding-doubling algorithm by Briegleb and Light (2007) is unsurpassed as a radiative transfer core. The evaluation in Section 5 shows that this algorithm produces the least error for snow albedo and solar absorption within snowpack, especially under overcast skies. This algorithm applies well to both uniformly refractive media such as snow on land, and to non-uniformly refractive media, such as bare/snow-covered/ponded sea ice and bare/snow-covered land ice. Numerical singularities occur only rarely (when $\mu_0 = 0$) and are easily avoided in model implementations. Among the three two-stream algorithms discussed here, dEdd-AD is also the most efficient one as it takes only ~2/3 of the time of SNICAR and 2SD to compute solar properties of multi-layer snowpacks.

Second, any two-stream cryospheric radiative transfer model can incorporate the parameterization described in Section 6 to adjust the low bias of direct near-IR snow albedo and high bias of direct near-IR solar absorption in snow, for solar zenith angles larger than 75°. These biases are persistent across all two-stream algorithms discussed in this work, and should be corrected for snow-covered surfaces. Alternatively, adopting a 4-stream approximation would reduce or eliminate such biases, though at considerable expense in computational efficiency.

Third, a cryospheric radiative transfer model should prefer physically based parameterizations that are extensible and convergent (e.g., with increasing spectral resolution) for the band-averaged SSPs and size distribution of snow. Although the treatments used in SNICAR and dEdd-AD are both practical since they both reproduce the narrowband solar properties with carefully derived band-averaged inputs as discussed in Section 7, the snow treatment used in SNICAR is more physically based and reproducible since it does not rely on subjective adjustment and empirical coefficients as used in dEdd-AD. Specifically, the empirical adjustment to snow grain radius implemented in dEdd-AD may not always produce compensating errors. For example, in snow containing light-absorbing impurities such adjustment may also lead to biases in aerosol absorption since the albedo reduction caused by light-absorbing particles does not linearly depend on snow grain radius (Dang et al., 2015). For further model development incorporating non-spherical snow grain shapes (Dang et al., 2016; He et al., 2018ab), such adjustment on grain radius may fail as well. Moreover, SNICAR computes the snow

Author
Deleted: y

Author
Deleted: the CICE radiative core

Author
Deleted: CICE

Author
Deleted: CICE

Author
Deleted: CICE

properties for four near-IR bands, which helps capture the spectral variation of albedo (Figure 1) and therefore better represents near-IR solar properties. It is also worth noting that unlike the radiative core of dEdd-AD, SNICAR is actively maintained with numerous modifications and updates in the past decade (e.g. Flanner et al., 2012; He et al., 2018b). Snow radiative treatments that follow SNICAR conventions for SSPs may take advantage of these updates. Note that any radiative core that follows SNICAR SSP conventions must be called twice to compute diffuse and direct solar properties, respectively.

Fourth, a surface cryospheric radiative transfer model should flexibly accommodate coupled simulations with distinct atmospheric and surface spectral grids. Both the 5-band scheme used in SNICAR and the 3-band scheme used in dEdd-AD separate the visible from near-IR spectrum at 0.7 µm. This boundary aligns with the Community Atmospheric Model's original radiation bands (CAM; Neale et al., 2012), though not with the widely used Rapid Radiative Transfer Model (RRTMG; Iacono et al., 2008) which places 0.7 µm squarely in the middle of a spectral band. A mismatch in spectral boundaries between atmospheric and surface radiative transfer schemes can require an ESM to unphysically apportion energy from the straddled spectral bin when coupling fluxes between surface and atmosphere. The spectral grids of surface and atmosphere radiation need not be identical so long as the coarser grid shares spectral boundaries with the finer grid. In practice maintaining a portable cryospheric radiative module such as SNICAR requires a complex offline toolchain (Mie solver, spectral refractive indices for air, water, ice, and aerosols, spectral solar insolation for clear and cloudy skies) to compute, integrate, and rebin SSPs. Aligned spectral boundaries between surface and atmospheric would simplify the development of efficient and accurate radiative transfer for the coupled Earth system.

Last, it is important to note that, although we only examine the performance of the dEdd-AD for pure snow in this work, this algorithm can be applied to the surface solar calculation of all cryospheric components with or without light-absorbing particles present. First, Briegleb and Light (2007) proved its accuracy for simulating ponded/bare sea-ice solar properties against observations and a Monte Carlo radiation model. Second, In CESM and E3SM, the radiative transfer simulation of snow on land ice is carried out by SNICAR with prescribed land ice albedo. Adopting dEdd-AD radiative core in SNICAR will permit these ESMs to couple the snow and land ice as a non-uniformly refractive column for more accurate solar computations since bare/snow-covered/ponded

Author
Deleted: Figure 2

Author
Deleted: CICE

Author
Deleted: CICE

Author
Deleted:

Author
Deleted: CICE

Author
Deleted: adding-doubling algorithm

Author
Deleted: the CICE

Author
Deleted: adding-doubling core

land ice is physically similar to bare/snow-covered/ponded sea ice, and the latter is already treated well by dEdd-AD radiative transfer core. Third, adding light-absorbing particles in snow will not change our results qualitatively. Both dEdd-AD and SNICAR simulate the impact of light-absorbing particles (black carbon and dust) on snow and/or sea ice using self-consistent particle SSPs that follow the SNICAR convention (e.g., Flanner et al., 2007; Holland et al. 2012). These particles are assumed to be either internally or externally mixed with snow crystals; the combined SSPs of mixtures (e.g. Appendix A of Dang et al., 2015) are then used as the inputs for radiative transfer calculation. The adoption of dEdd-AD radiative transfer algorithm in SNICAR, and the implementation of SNICAR snow SSPs in dEdd-AD enables a consistent simulation of the radiative effects of light-absorbing particles in the cryosphere across ESM components.

In summary, this inter-comparison and evaluation has shown multiple ways that the solar properties of cryospheric surfaces can be improved in the current generation of ESMs. We have merged these findings into a hybrid model SNICAR-AD, which is primarily composed of the radiative transfer scheme of dEdd-AD, 5-band snow/aerosol SSPs of SNICAR, and the parameterization to correct for snow albedo biases when solar zenith angle exceeds 75°. This hybrid model can be applied to snow on land, land ice, and sea ice to produce consistent shortwave radiative properties for snow-covered surfaces across the Earth system. With the evolving and further understanding of snow and aerosol physics and chemistry, the adoption of this hybrid model will obviate the effort to modify and maintain separate optical variable input files used for different model components.

SNICAR-AD is now implemented in both the sea-ice (MPAS-seaice) and land (ELM) components of E3SM. More simulations and analyses are underway to examine its impact on E3SM model performance and simulated climate. The results are however beyond the scope of this work and will be thoroughly discussed in a future paper.

9. Conclusions

In this work, we aim to improve and unify the solar radiative transfer calculations for snow on land and snow on sea ice in ESMs by evaluating the following two-stream radiative transfer algorithms: the two-stream delta-Eddington adding-doubling algorithm dEdd-AD implemented in sea-ice model Icepack/CICE/MPAS-seaice, the two-stream delta-Eddington and two-stream delta-Hemispheric-Mean algorithms implemented in snow model SNICAR, and a two-stream delta-Discrete-Ordinate algorithm. Among these three models, the dEdd-AD produces the most accurate snow albedo and solar absorption

Author
Deleted: CICE

Author
Deleted: CICE

Author
Formatted: None, Font:(Default) Times, Underline color: Blue, Font color: Black

Author
Deleted: .

Author
Deleted: CICE

Author
Deleted: CICE

Author
Deleted: will enable

Author
Deleted: n

Author
Deleted: We have adopted these recommendations in a hybrid model SNICAR-AD, implemented in MPAS-seaice and E3SM Land Model (ELM), to examine the response of climate to this improved and unified cryospheric surface radiation treatment in future E3SM studies.

Author
Deleted:

Author
Deleted: two-stream delta-Eddington adding-doubling algorithm

(Section 5). All two-stream models underestimate near-IR snow albedo and overestimate near-IR absorption when solar zenith angles are larger than 75°, which can be adjusted by a parameterization we developed (Section 6). We compared the implementations of radiative transfer cores in SNICAR and dEdd-AD (Section 7) and recommended a consistent and hybrid shortwave radiative model SNICAR-AD for snow-covered surfaces across ESMs (Section 8). Improved treatment of surface cryospheric radiative properties in the thermal infrared has recently been shown to remediate significant climate simulation biases in Polar Regions (Huang et al., 2018). It is hoped that adoption of improved and consistent treatments of solar radiative properties for snow-covered surfaces as described in this study will further remediate simulation biases in snow-covered regions.

Author
Deleted: CICE

Author
Deleted: treatment

Author
Deleted: (i.e. the hybrid model SNICAR-AD)

Author
Deleted: Polar Regions.

Data availability. The data and models are available upon request to Cheng Dang (cdang5@uci.edu). SNICAR and dEdd-AD radiative transfer core can be found at https://github.com/E3SM-Project/E3SM.

Competing interests. The authors declare that they have no conflict of interest.

Acknowledgments. The authors thank Prof. Stephen G. Warren and Prof. Qiang Fu for insightful discussions on radiative transfer algorithms. The authors thank Dr. Adrian Turner for instructions on installing and running MPAS-seaice. The authors thank Dr. David Bailey and one anonymous reviewer for their careful reading and insightful suggestions. This research is supported as part of the Energy Exascale Earth System Model (E3SM) project, funded by the U.S. Department of Energy, Office of Science, Office of Biological and Environmental Research, with funding number DE-SC0012998.

References

Aoki, T., Kuchiki, K., Niwano, M., Kodama, Y., Hosaka, M. and Tanaka, T.: Physically based snow albedo model for calculating broadband albedos and the solar heating profile in snowpack for general circulation models. Journal of Geophysical Research, 116, D11114, https://doi.org/10.1029/2010JD015507, 2011.

Bøggild, C.E., Brandt, R.E., Brown, K.J. and Warren, S.G.: The ablation zone in northeast Greenland: ice types, albedos and impurities. Journal of Glaciology, 56, 101-113, pp.101-113, https://doi.org/10.3189/002214310791190776, 2010.

Brandt, R.E., Warren, S.G., Worby, A.P. and Grenfell, T.C.: Surface albedo of the Antarctic sea ice zone. Journal of Climate, 18(17), pp.3606-3622. https://doi.org/10.1175/JCLI3489.1 2005.

Briegleb, P. and Light, B.: A Delta-Eddington mutiple scattering parameterization for solar radiation in the sea ice component of the community climate system model, 2007.

Dang, C. and Hegg, D.A.: Quantifying light absorption by organic carbon in Western North American snow by serial chemical extractions. Journal of Geophysical Research, 119(17), pp.10-247. https://doi.org/10.1002/2014JD022156, 2014.

Dang, C., Fu, Q. and Warren, S.G., 2016. Effect of snow grain shape on snow albedo. Journal of the Atmospheric Sciences, 73(9), pp.3573-3583. https://doi.org/10.1175/JAS-D-15-0276.1, 2016.

Dang, C., Brandt, R.E. and Warren, S.G.: Parameterizations for narrowband and broadband albedo of pure snow and snow containing mineral dust and black carbon. Journal of Geophysical Research: Atmospheres, 120(11), pp.5446-5468, https://doi.org/10.1002/2014JD022646, 2015.

Dang, C., Warren, S.G., Fu, Q., Doherty, S.J., Sturm, M. and Su, J.: Measurements of light-absorbing particles in snow across the Arctic, North America, and China: Effects on surface albedo. Journal of Geophysical Research: Atmospheres, 122(19), pp.10-149. https://doi.org/10.1002/2017JD027070, 2017.

Author
Deleted: CICE

Author
Deleted: e

Author
Deleted: helpful

Author
Deleted: was

Author
Deleted: DOE BER ESM (

Author
Deleted:)

Doherty, S.J., Hegg, D.A., Johnson, J.E., Quinn, P.K., Schwarz, J.P., Dang, C. and Warren, S.G.: Causes of variability in light absorption by particles in snow at sites in Idaho and Utah. Journal of Geophysical Research: Atmospheres, 121(9), pp.4751-4768. https://doi.org/10.1002/2015JD024375, 2016.

Doherty, S.J., Warren, S.G., Grenfell, T.C., Clarke, A.D. and Brandt, R.E.: Light-absorbing impurities in Arctic snow. Atmospheric Chemistry and Physics. 10(23), pp.11647-11680. https://doi.org/10.5194/acp-10-11647-2010, 2010.

Doherty, S.J., Dang, C., Hegg, D.A., Zhang, R. and Warren, S.G.: Black carbon and other light-absorbing particles in snow of central North America. Journal of Geophysical Research: Atmospheres, 119(22), pp.12-807, https://doi.org/10.1002/2014JD022350, 2014.

Flanner, M.G. and Zender, C.S.: Snowpack radiative heating: Influence on Tibetan Plateau climate. Geophysical Research Letters, 32(6). https://doi.org/10.1029/2004GL022076, 2005.

Flanner, M.G., Zender, C.S., Randerson, J.T. and Rasch, P.J.: Present-day climate forcing and response from black carbon in snow. Journal of Geophysical Research: Atmospheres, 112(D11). https://doi.org/10.1029/2006JD008003, 2007.

Flanner, M.G., Liu, X., Zhou, C., Penner, J.E. and Jiao, C.: Enhanced solar energy absorption by internally-mixed black carbon in snow grains. Atmospheric Chemistry and Physics, 12(10), pp.4699-4721. https://doi.org/10.5194/acp-12-4699-2012, 2012.

Gardner, A.S. and Sharp, M.J.: A review of snow and ice albedo and the development of a new physically based broadband albedo parameterization. Journal of Geophysical Research: Earth Surface, 115(F1). https://doi.org/10.1029/2009JF001444, 2010.

Grenfell, T.C., Neshyba, S.P. and Warren, S.G.: Representation of a nonspherical ice particle by a collection of independent spheres for scattering and absorption of radiation: 3. Hollow columns and plates. Journal of Geophysical Research: Atmospheres, 110(D17). https://doi.org/10.1029/2005JD005811, 2005.

He, C., Liou, K.N., Takano, Y., Yang, P., Qi, L. and Chen, F.: Impact of grain shape and multiple black carbon internal mixing on snow albedo: Parameterization and radiative effect analysis. Journal of Geophysical Research: Atmospheres, 123(2), pp.1253-1268. https://doi.org/10.1002/2017JD027752, 2018a.

He, C., Flanner, M.G., Chen, F., Barlage, M., Liou, K.N., Kang, S., Ming, J. and Qian, Y.: Black carbon-induced snow albedo reduction over the Tibetan Plateau: uncertainties from snow grain shape and aerosol–snow mixing state based on an updated SNICAR model. Atmospheric Chemistry and Physics, 18, pp.11507-11527. https://doi.org/10.5194/acp-18-11507-2018, 2018b.

He, C., Takano, Y., Liou, K.N., Yang, P., Li, Q. and Chen, F.: Impact of Snow Grain Shape and Black Carbon–Snow Internal Mixing on Snow Optical Properties: Parameterizations for Climate Models. Journal of Climate, 30(24), pp.10019-10036. https://doi.org/10.1175/JCLI-D-17-0300.1, 2017.

Holland, M.M., Bailey, D.A., Briegleb, B.P., Light, B. and Hunke, E.: Improved sea ice shortwave radiation physics in CCSM4: The impact of melt ponds and aerosols on

Arctic sea ice. Journal of Climate, 25(5), pp.1413-1430. https://doi.org/10.1175/JCLI-D-11-00078.1, 2012.

Huang, X., Chen, X., Flanner, M., Yang, P., Feldman, D. and Kuo, C.: Improved representation of surface spectral emissivity in a global climate model and its impact on simulated climate. Journal of Climate, 31(9), pp.3711-3727. https://doi.org/10.1175/JCLI-D-17-0125.1, 2018.

Hunke, E. C., Lipscomb, W. H., Turner, A. K., Jeffery, N., and Elliott, S.: CICE: the Los Alamos Sea Ice Model Documentation and Software User's Manual Version 4.1 LA-CC-06-012. T-3 Fluid Dynamics Group, Los Alamos National Laboratory 675. 2010.

Iacono, M.J., Delamere, J.S., Mlawer, E.J., Shephard, M.W., Clough, S.A. and Collins, W.D.: Radiative forcing by long-lived greenhouse gases: Calculations with the AER radiative transfer models. Journal of Geophysical Research: Atmospheres, 113(D13), https://doi.org/10.1029/2008JD009944, 2008.

Jin, Z. and Stamnes, K.: Radiative transfer in nonuniformly refracting layered media: atmosphere–ocean system. Applied Optics, 33(3), pp.431-442. https://doi.org/10.1364/AO.33.000431, 1994.

Kuipers Munneke, P., Van den Broeke, M.R., Lenaerts, J.T.M., Flanner, M.G., Gardner, A.S. and Van de Berg, W.J.: A new albedo parameterization for use in climate models over the Antarctic ice sheet. Journal of Geophysical Research: Atmospheres, 116(D5). https://doi.org/10.1029/2010JD015113, 2011.

Lee, W.L. and Liou, K.N.: A coupled atmosphere–ocean radiative transfer system using the analytic four-stream approximation. Journal of the Atmospheric Sciences, 64(10), pp.3681-3694. https://doi.org/10.1175/JAS4004.1, 2007.

Liang, S., Fang, H., Chen, M., Shuey, C.J., Walthall, C., Daughtry, C., Morisette, J., Schaaf, C. and Strahler, A.: Validating MODIS land surface reflectance and albedo products: Methods and preliminary results. Remote sensing of environment, 83(1-2), pp.149-162. https://doi.org/10.1016/S0034-4257(02)00092-5, 2002.

Light, B., Grenfell, T. C. and Perovich, D.K.: Transmission and absorption of solar radiation by Arctic sea ice during the melt season. Journal of Geophysical Research: Oceans 113, no. C3, https://doi.org/10.1029/2006JC003977, 2008.

Light, B., Perovich, D.K., Webster M.A., Polashenski, C., and Dadic, R.: Optical properties of melting first-year Arctic sea ice. Journal of Geophysical Research: Oceans 120, no. 11: 7657-7675, https://doi.org/10.1002/2015JC011163, 2015.

Marshall, S. and Oglesby, R.J.: An improved snow hydrology for GCMs. Part 1: Snow cover fraction, albedo, grain size, and age. Climate Dynamics, 10(1-2), pp.21-37. https://doi.org/10.1007/BF00210334, 1994.

Marshall, S.E.: A Physical Parameterization of Snow Albedo for Use in Climate Models, NCAR Cooperative Thesis 123, National Center for Atmospheric Research, Boulder, CO, 175 pp. 1989.

Matzl, M. and Schneebeli, M.: Measuring specific surface area of snow by near-infrared photography. Journal of Glaciology, 52(179), pp.558-564. https://doi.org/10.3189/172756506781828412, 2006.

Matzl, M. and Schneebeli, M.: Stereological measurement of the specific surface area of seasonal snow types: Comparison to other methods, and implications for mm-scale vertical profiling. Cold Regions Science and Technology, 64(1), pp.1-8. https://doi.org/10.1016/j.coldregions.2010.06.006, 2010.

Meador, W.E. and Weaver, W.R.: Two-stream approximations to radiative transfer in planetary atmospheres: A unified description of existing methods and a new improvement. Journal of the Atmospheric Sciences, 37(3), pp.630-643. https://doi.org/10.1175/1520-0469(1980)037<0630:TSATRT>2.0.CO;2, 1980.

Mlawer, E.J. and Clough, S.A.: On the extension of rapid radiative transfer model to the shortwave region. In Proceedings of the 6th Atmospheric Radiation Measurement (ARM) Science Team Meeting, US Department of Energy, CONF-9603149, 223–226. 1997.

Neale, Richard B., Chen, C.-C., Gettelman, A., Lauritzen, P. H., Park, S., Williamson, D. L., Conley, A. J., Garcia, R., Kinnison, D., Lamarque, J. F., and Marsh, D.: Description of the NCAR community atmosphere model (CAM 5.0). NCAR Tech. Note NCAR/TN-486+ STR 1, no. 1: 1-12. 2010.

Neshyba, S.P., Grenfell, T.C. and Warren, S.G.: Representation of a nonspherical ice particle by a collection of independent spheres for scattering and absorption of radiation: 2. Hexagonal columns and plates. Journal of Geophysical Research: Atmospheres, 108(D15). https://doi.org/10.1029/2002JD003302, 2003.

Perovich, D. K.: The optical properties of sea ice (No. MONO-96-1). COLD REGIONS RESEARCH AND ENGINEERING LAB HANOVER NH. 1996.

Stamnes, K., Tsay, S.C., Wiscombe, W. and Jayaweera, K.: Numerically stable algorithm for discrete-ordinate-method radiative transfer in multiple scattering and emitting layered media. Applied optics, 27(12), pp.2502-2509. https://doi.org/10.1364/AO.27.002502, 1988.

Thomas, G.E. and K. Stamnes (1999), Radiative transfer in the atmosphere and ocean. Cambridge University Press.

Toon, O. B., McKay, C. P., Ackerman, T. P., and Santhanam, K.: Rapid calculation of radiative heating rates and photodissociation rates in inhomogeneous multiple scattering atmospheres, J. Geophys. Res., 94(D13), 16,287–16,301. https://doi.org/10.1029/JD094iD13p16287, 1989.

Turner, A.K., Lipscomb, W.H., Hunke, E.C., Jacobsen, D.W., Jeffery, N., Ringler, T.D. and Wolfe, J.D.: MPAS-Seaice: a new variable resolution sea-ice model. J. Adv. Model Earth Sy., in preparation., 2018.

Wang, X., Doherty, S.J. and Huang, J.: Black carbon and other light‐absorbing impurities in snow across Northern China. Journal of Geophysical Research: Atmospheres, 118(3), pp.1471-1492. https://doi.org/10.1029/2012JD018291, 2013.

Warren, S. G.: Optical properties of snow. Reviews of Geophysics 20, no. 1: 67-89. https://doi.org/10.1029/RG020i001p00067,1982.

Warren, S.G. and Wiscombe, W.J.: A model for the spectral albedo of snow. II: Snow containing atmospheric aerosols. Journal of the Atmospheric Sciences, 37(12), pp.2734-2745.https://doi.org/10.1175/1520-0469(1980)037<2734:AMFTSA>2.0.CO;2, 1980

Warren, S.G. and Brandt, R.E.: Optical constants of ice from the ultraviolet to the microwave: A revised compilation. Journal of Geophysical Research: Atmospheres, 113(D14). https://doi.org/10.1029/2007JD009744, 2008.

Warren, S.G. and Wiscombe, W.J.: Dirty snow after nuclear war. Nature, 313(6002), p.467. https://doi.org/10.1038/313467a0, 1985.

Wiscombe, W. J.: The delta-Eddington approximation for a vertically inhomogeneous atmosphere, NCAR Tech. Note TN-140_STR [NTIS P6270618]. 1977.

Wiscombe, W.J.: Improved Mie scattering algorithms. Applied optics, 19(9), pp.1505-1509. https://doi.org/10.1364/AO.19.001505,1980.

Wiscombe, W.J. and Warren, S.G.: A model for the spectral albedo of snow. I: Pure snow. Journal of the Atmospheric Sciences, 37(12), pp.2712-2733. https://doi.org/10.1175/1520-0469(1980)037<2712:AMFTSA>2.0.CO;2, 1980.

Zender, C.S.: Global climatology of abundance and solar absorption of oxygen collision complexes. Journal of Geophysical Research: Atmospheres, 104(D20), pp.24471-24484. https://doi.org/10.1029/1999JD900797, 1999.

Zender, C.S., Bush, B., Pope, S.K., Bucholtz, A., Collins, W.D., Kiehl, J.T., Valero, F.P. and Vitko Jr, J.: Atmospheric absorption during the atmospheric radiation measurement (ARM) enhanced shortwave experiment (ARESE). Journal of Geophysical Research: Atmospheres, 102(D25), pp.29901-29915. https://doi.org/10.1029/97JD01781, 1997.

Figure 1. The spectral albedo of pure snow computed using 16-stream DISORT, SNICAR, dEdd-AD, and 2SD models, for clear-sky (direct beam at solar zenith angle 60°) and cloudy-sky conditions in the left and right panels, respectively. The top panels show spectral albedo. The middle panels show the difference ($\delta\alpha = \alpha_2 - \alpha_{16}$) in spectral albedos computed using the two-stream model (α_2) and 16-stream DISORT (α_{16}). The bottom panels show the difference of reflected spectral flux given $\delta\alpha$. The snowpack is set to semi-infinite deep with grain radius of 100 μm.

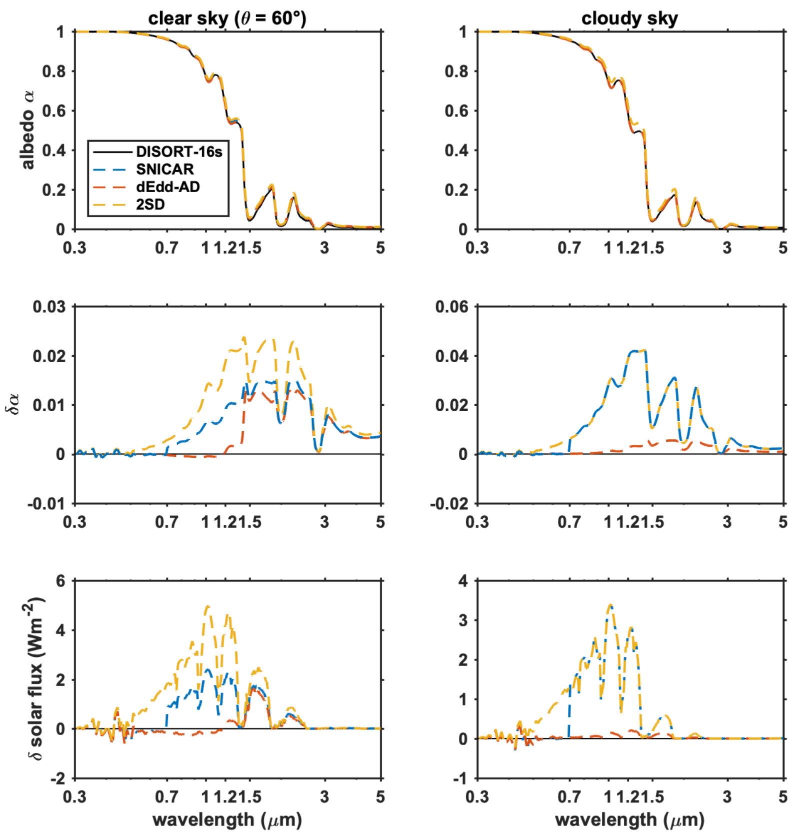

Author
Deleted: CICE

Figure 2. Spectral and total down-welling solar flux at surface computed using SWNB2 for (a) standard clear-sky and cloudy-sky atmospheric profiles of mid-latitude winter assuming solar zenith angle is 60° at the top of the atmosphere, and for (b) standard clear sky profiles of mid-latitude and sub-Arctic winter with different incident solar zenith angles.

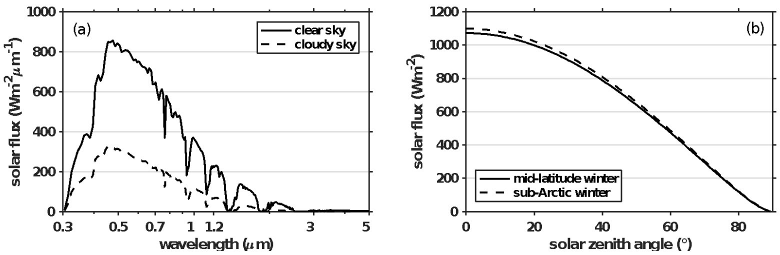

Figure 3. The difference in direct snow albedo ($\delta\alpha = \alpha_2 - \alpha_{16}$) computed using two-stream models (α_2) and using 16-stream DISORT model (α_{16}), for various snow depths and solar zenith angles, with snow grain radius of 100 µm. From the top to the bottom rows are results of two-stream models SNICAR, dEdd-AD, and 2SD. From the left to the right columns are albedo differences of all-wave, visible, near-IR bands.

Author
Deleted: CICE

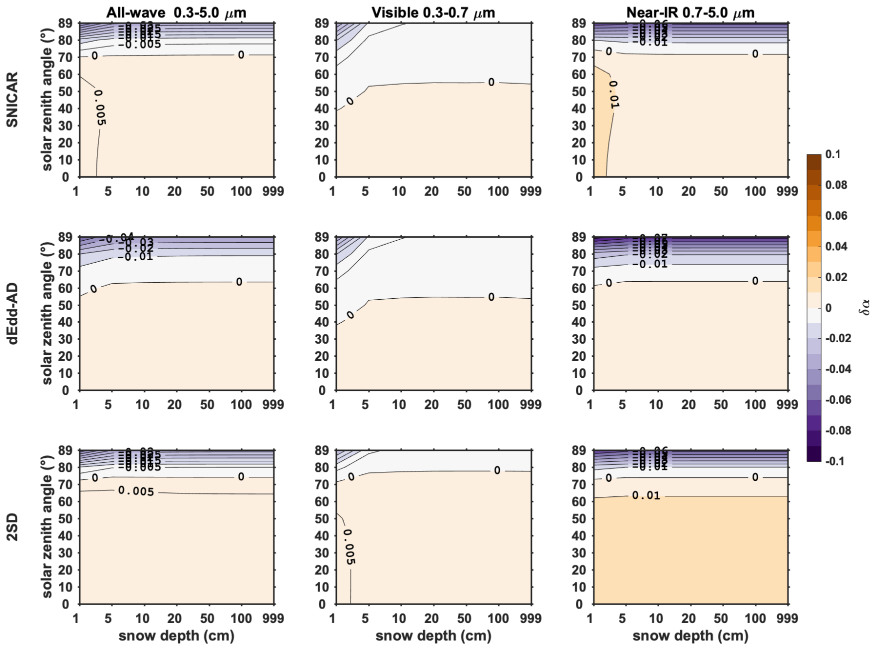

Figure 4. The difference in direct snow albedo ($\delta\alpha = \alpha_2 - \alpha_{16}$) computed using two-stream models (α_2) and using 16-stream DISORT model (α_{16}), for various snow depths and solar zenith angles, with snow grain radius of 1000 µm.

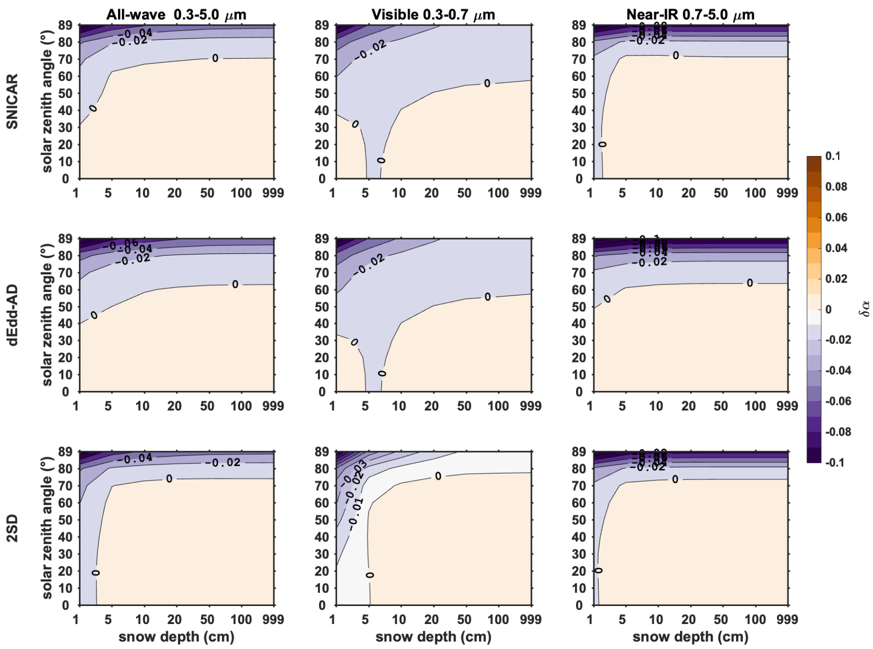

Author
Deleted: The same to Figure 3

Author
Deleted: , but for snow grain radius of

Figure 5. The difference in direct snow albedo ($\delta\alpha = \alpha_2 - \alpha_{16}$) computed using two-stream models (α_2) and using 16-stream DISORT model (α_{16}), for various snow depths and snow grain radii, with solar zenith angle of 60°.

Author
Deleted: The same to Figure 3, but for fixed

Author
Deleted: and different snow grain radii

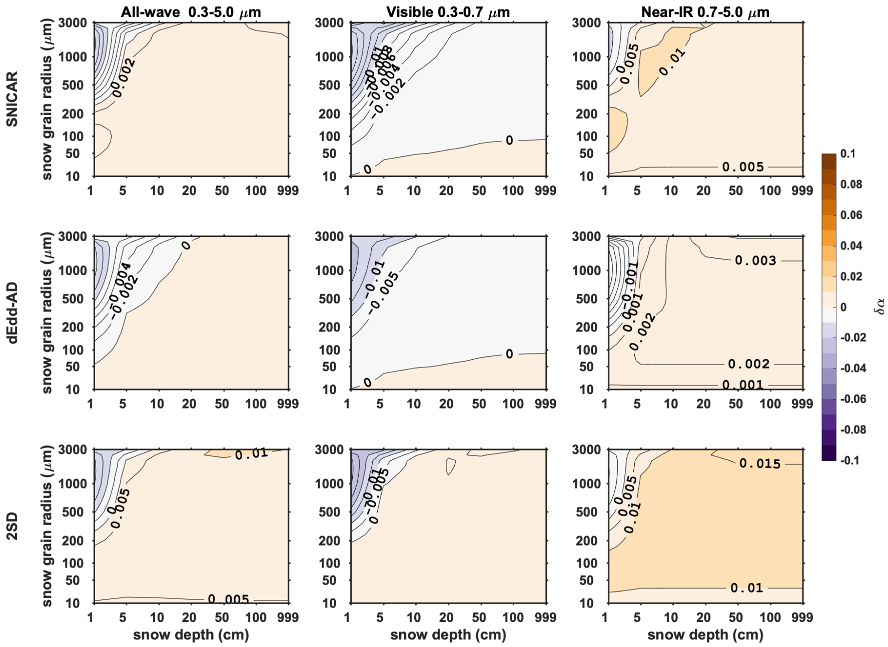

Figure 6. The difference in diffuse snow albedo ($\delta\alpha = \alpha_2 - \alpha_{16}$) computed using two-stream models (α_2) and using 16-stream DISORT model (α_{16}), for various snow depths and snow grain radii, with solar zenith angle of 60° at the top of the atmosphere.

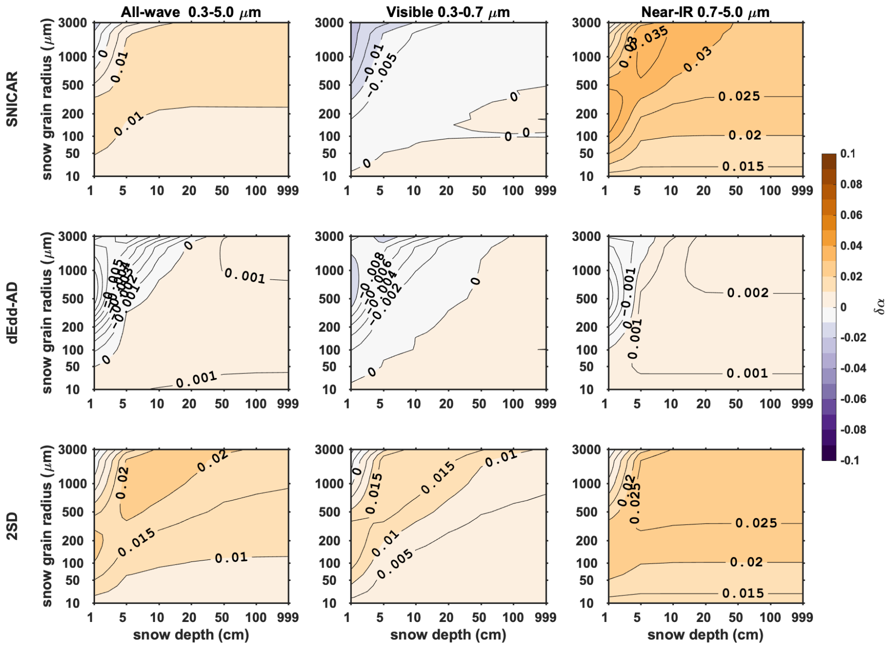

Author
Deleted: The same to Figure 5, but for diffuse snow albedo with different snow grain radii.

Figure 7. Error in reflected direct solar flux given albedo errors shown in Figure 3.

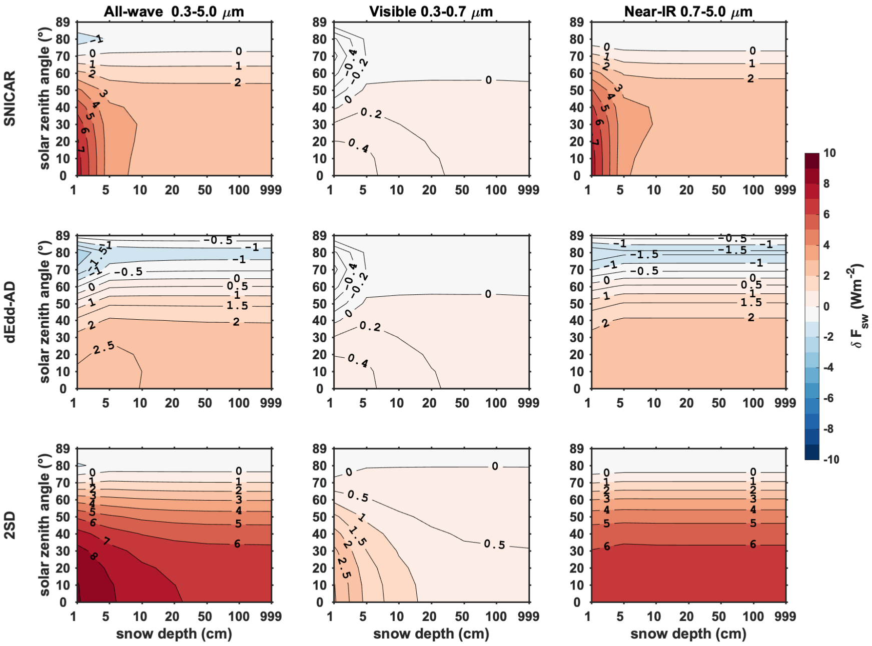

Figure 8. Error in reflected direct solar flux given albedo errors shown in Figure 4.

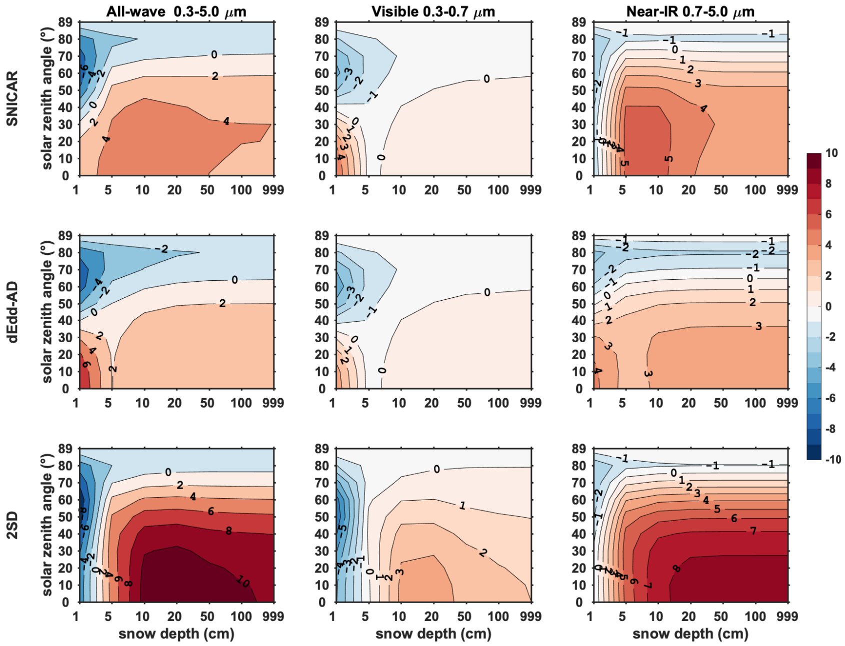

Figure 9. Error in reflected diffuse solar flux given albedo errors shown in Figure 6.

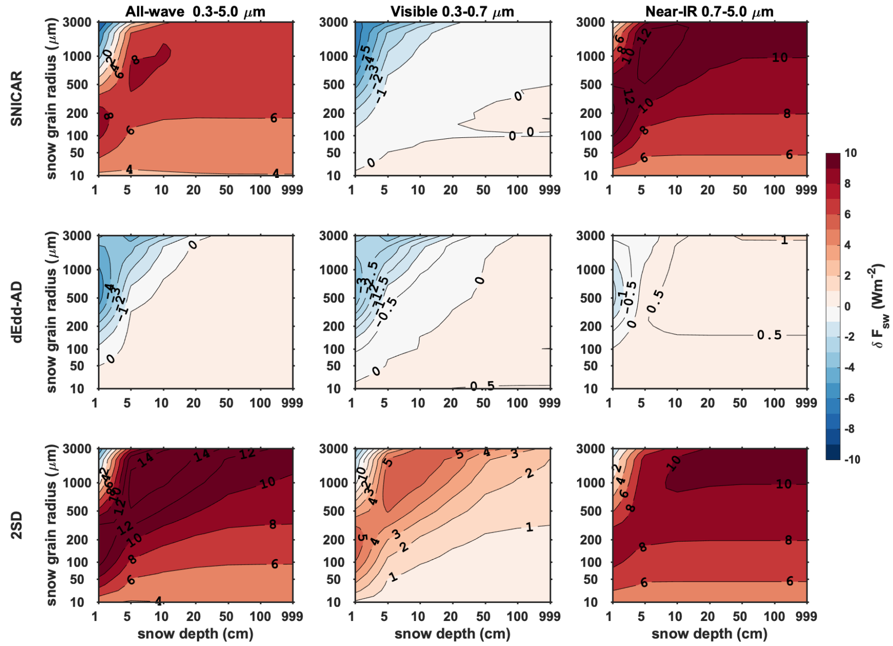

Figure 10. Comparison of light-absorption profiles derived from two-stream models and 16-stream DISORT. The left-most column shows fractional band absorptions computed using 16-stream DISORT. The right three panels show the errors of all-wave, visible, and near-IR fractional absorptions calculated using two-stream models. The top and bottom panels are for clear-sky and cloudy-sky conditions (solar zenith angle of 60°), respectively. The snowpack is 10 cm deep and is divided evenly into five 2-cm thick layers, for new snow (r = 100 μm) and old snow (r = 1000 μm). The layers 1-4 represent the top four snow layers (top 8 cm), and layer 5 represents underlying ground with albedo of 0.25.

Author
Deleted: ,

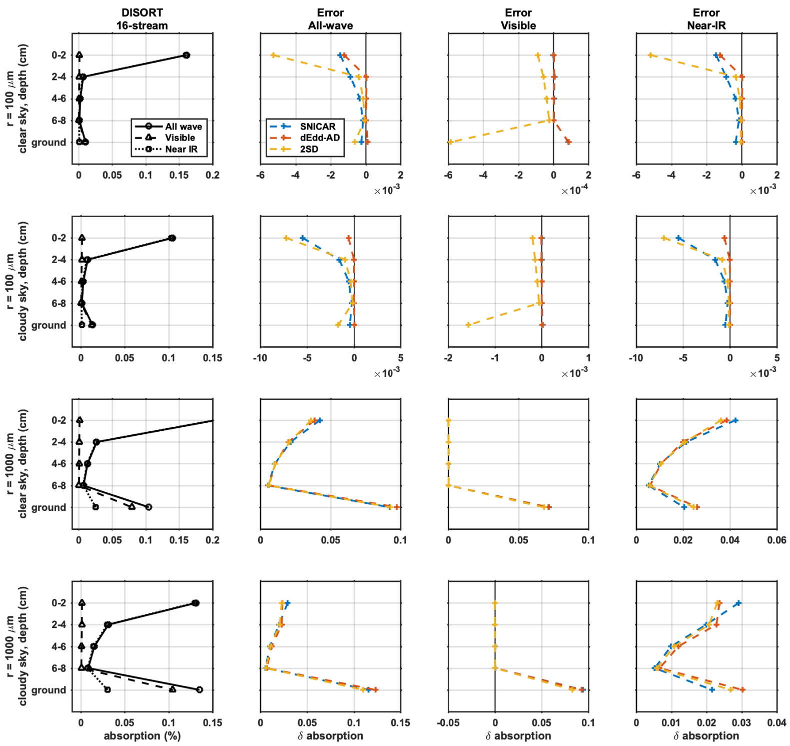

Figure 11. (a) Direct near-IR snow albedo and (b) near-IR fractional absorption by top 2-cm snow of a 2-m thick snowpack, for solar zenith angles larger than 70° and snow grain radii of 100 µm and 1000 µm. (c) The ratios of near-IR albedo computed using CICE to that computed using 16-stream DISORT for different solar zenith angles. These ratios are parameterized as linear functions of the logarithmic of snow grain radius. The slopes and y-intercepts are shown in (d). The black dashed curves in figures (c) and (d) are fitting values computed using parameterization discussed in Section 5.

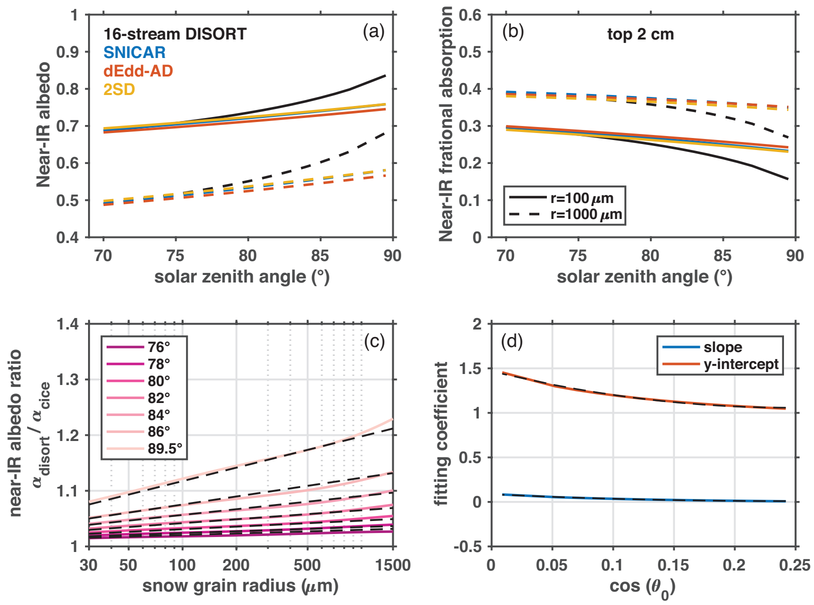

Figure 12. Error in semi-infinite snow albedo computed using dEdd-AD before (top row) and after (bottom row) incorporating corrections for near-IR albedo, for different solar zenith angles and snow grain radii.

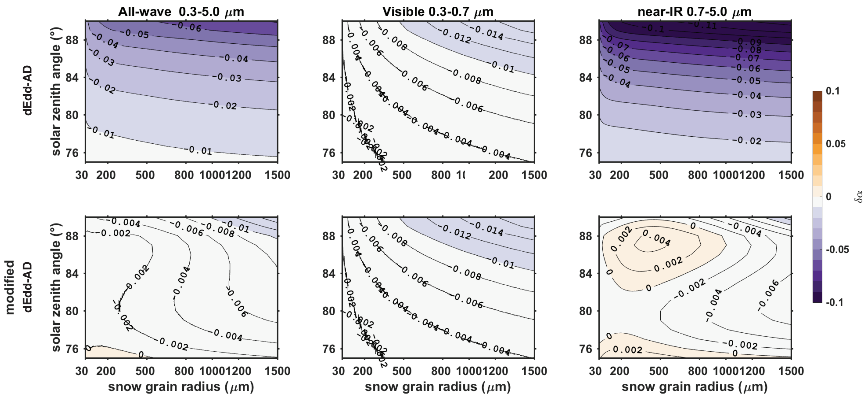

Author
Deleted: CICE

Table 1. Acronyms used in this paper and their references.

ESM/ESMs	Earth System Models	
E3SM	Energy Exscale Earth System Model	Global climate model, previously know as ACME, https://e3sm.org/
CESM	Community Earth System Model	Global climate model, http://www.cesm.ucar.edu/
CCSM	Community Climate System Model	Global climate model, http://www.cesm.ucar.edu/models/ccsm4.0/
RACMO	Regional Atmospheric Climate Model	Regional model, https://www.projects.science.uu.nl/iceclimate/models/racmo.php
CAM	Community Atmospheric Model	Atmospheric model, Neale et al., 2012
ELM	E3SM land model	Land model of E3SM, https://e3sm.org/model/e3sm-model-description/v1-description/
CLM	Community land model	Land model of CESM, http://www.cesm.ucar.edu/models/clm/
MPAS-seaice	Model for Prediction Across Scales Sea Ice	Sea-ice model of E3SM, Turner et al., 2018
CICE	Los Almos Sea Ice Model	Sea-ice model of CESM, Hunke et al., 2010
RRTM	Rapid Radiative Transfer Model	Standalone column radiative transfer model, Mlawer and Clough, 1997, http://rtweb.aer.com/rrtm_frame.html
RRTMG	Rapid Radiative Transfer Model for GCM components	Modified RRTM for GCM application, Iacono et al., 2008, http://rtweb.aer.com/rrtm_frame.html
DISORT	DIScrete-Odinate Radiative Transfer model	Standalone column radiative transfer model, http://lllab.phy.stevens.edu/disort/, Stamnes et al., 1988
SWNB2	Shortwave Narrowband Model	Standalone column radiative transfer model, Zender et al., 1997; Zender, 1999
SNICAR	SNow ICe and Aerosol Radiative module	Snow module used in ELM and CLM, Flanner and Zender, 2005; Toon et al., 1989

dEdd-AD	Two-stream delta-Eddington Adding-Doubling radiative transfer algorithm	Sea-ice radiative transfer core in MPAS-seaice and CICE, Briegleb and Light, 2007
2SD	Two-Stream Discrete ordinate radiative transfer algorithm	Radiative transfer algorithm tested in this work, Jin and Stamnes, 1994
SNICAR-AD	SNICAR – Adding Doubling	Hybrid snow/sea-ice radiative transfer model, Section 8
SSP/SSPs	Single-Scattering Properties	Single-scattering albedo ϖ, asymmetry factor g, extinction coefficient σ_{ext}
near-IR	Near Infrared band	Wavelengths of 0.7 - 5 μm

Table 2. Two-stream radiative transfer algorithms evaluated in this work, including algorithms that are currently implemented in Earth System Model CESM and E3SM.

Author
Deleted: 1

ESM Component	Land	Sea Ice	
Model	SNICAR	dEdd-AD	2SD
Radiative transfer approximation	two-stream δ-Eddington (visible) δ-Hemispheric-mean (near-IR)	two-stream δ-Eddington	two-stream δ-Discrete-ordinate
Treatment for multi-layered media	matrix inversion	adding-doubling	matrix inversion
Fresnel reflection/refraction	no	yes	yes
Number of bands implemented in ESMs	5 bands (1 visible, 4 near-IR)	3 bands (1 visible, 2 near-IR)	
Applies to	snow	bare/ponded/snow-covered sea ice, and snow	bare/ponded/snow-covered sea ice, and snow

Author
Deleted: CICE/MPAS-seaice